~~SECURITY INFORMATION~~

~~CONFIDENTIAL~~

Copy 235
RM L52E19

NACA RM L52E19

7338

TECH LIBRARY KAFB, NM
0144368

NACA

RESEARCH MEMORANDUM

A THEORETICAL INVESTIGATION OF THE EFFECT OF A TARGET SEEKER SENSITIVE TO PITCH ATTITUDE ON THE DYNAMIC STABILITY AND RESPONSE CHARACTERISTICS OF A SUPERSONIC CANARD MISSILE CONFIGURATION

By Ordway B. Gates, Jr. and Albert A. Schy

Langley Aeronautical Laboratory
Langley Field, Va.

[redacted]

This material contains information affecting the National Defense of the United States within the meaning of the espionage [redacted] the transmission or revelation of which in any [redacted] to an unauthorized person is prohibited by law.

NATIONAL ADVISORY COMMITTEE
FOR AERONAUTICS

WASHINGTON

August 26, 1952

~~CONFIDENTIAL~~

Classification cancelled (or changed to Unclassified)

By Authority of NASA Tech Pub Announcement 74 30 Nov 54
(OFFICER AUTHORIZED TO CHANGE)

By .....
NAME

NK
GRADE OF OFFICER MAKING CHANGE)

10 Apr 61
DATE

TECH LIBRARY KAFB, NM
0144368

NATIONAL ADVISORY COMMITTEE FOR AERONAUTICS

RESEARCH MEMORANDUM

A THEORETICAL INVESTIGATION OF THE EFFECT OF A TARGET SEEKER SENSITIVE TO PITCH ATTITUDE ON THE DYNAMIC STABILITY AND RESPONSE CHARACTERISTICS OF A SUPERSONIC CANARD MISSILE CONFIGURATION

By Ordway B. Gates, Jr. and Albert A. Schy

SUMMARY

A theoretical investigation has been made of the longitudinal dynamic characteristics of an automatically stabilized supersonic canard missile configuration equipped with a target seeker sensitive to changes in pitch attitude. The effects of seeker gain, time delay, and nonlinearities, which include various types of dead spots in the seeker, are considered. The motions of the missile subsequent to command inputs or to an applied pitching moment were obtained by use of the Reeves Electronic Analog Computer.

The results indicated that time delays of the order investigated did not introduce large effects on the transient motions of the missile. Dead spots in the seeker resulted in steady-state errors subsequent to command or regulatory inputs, which for the command inputs increased with the size of the assumed dead spot. For a nonlinearity which effectively results in the seeker having a different gain constant for small errors than for large errors, the general effect was to give the system different degrees of stability throughout the course of the transient motions.

INTRODUCTION

As part of the general research program of missile automatic stabilization and control, a theoretical investigation has been made of the dynamic longitudinal performance characteristics of an automatically stabilized canard missile configuration equipped with an attitude-sensitive target-seeking device. The type of navigation system with which this control system is intended to be used is pursuit navigation.

AFB16

Since the primary purpose of this investigation was to determine the effect of dead spot and time delay in the target seeker on the longitudinal stability and response characteristics of the missile, the analysis has been made for a specific flight condition. The dynamic characteristics of the components of the system (fig. 1) with the exception of the target seeker, were obtained from references 1 and 2 which dealt with the normal acceleration and pitch-rate feedbacks, respectively. The results presented show the effects of the following on the longitudinal stability and response characteristics of the target-seeker-equipped missile configuration:

(1) Variation of target-seeker gain

(2) Time delay in target-seeker response

(3) Various types of dead spots in the target seeker

The longitudinal motions of the missile subsequent to command inputs and to an applied pitching moment were obtained by use of the Reeves Electronic Analog Computer.

SYMBOLS

I_Y	moment of inertia about Y stability axis, slug-ft^2
m	mass of missile, slugs
$\bar{c}$	mean aerodynamic chord, ft
S	wing area, sq ft
q	$\dot{\theta}\bar{c}/2V$ when used as a subscript
q	dynamic pressure, lb/sq ft
V	missile forward velocity, ft/sec
ξ	damping ratio of rate stabilization system
ω_n	natural frequency of rate stabilization system
ω	frequency, radians/sec
K_r	rate-stabilization-system gain constant, radians/radian/sec

K_1 target-seeker gain constant, g/radian

K_2 integrating-servo gain constant, radians/sec/g

τ target-seeker time constant, sec

n_o normal acceleration of missile, g units

n_i normal acceleration of missile called for by target seeker, g units

ϵ_1 attitude error, $\epsilon_1 = \theta_i - \theta_o$, radians

ϵ_2 normal acceleration error, $\epsilon_2 = n_i - n_o$, g units

g acceleration due to gravity, ft/sec^2

θ_i angle of pitch called for by target seeker, radians unless otherwise specified

θ_o angle of pitch, radians unless otherwise specified

α_o angle of attack, radians unless otherwise specified

γ_o flight-path angle, $\gamma_o = \theta_o - \alpha_o$, radians unless otherwise specified

δ canard-control-surface deflection, $\delta = \delta_s - \delta_R$, radians unless otherwise specified

δ_R control deflection due to rate servo, radians

δ_s control deflection due to integrating servo

t time, sec

M Mach number

C_L trim lift coefficient, $\frac{\text{Lift}}{qS}$

C_m pitching-moment coefficient, $\frac{\text{Pitching moment}}{qS\bar{c}}$

$C_{L_\delta} = \frac{\partial C_L}{\partial \delta}$

$C_{L_\alpha} = \frac{\partial C_L}{\partial \alpha}$

$C_{m_\delta} = \frac{\partial C_m}{\partial \delta}$

$C_{m_\alpha} = \frac{\partial C_m}{\partial \alpha}$

$C_{m_{\dot{\alpha}}} = \frac{\partial C_m}{\partial \frac{\dot{\alpha}\bar{c}}{2V}}$

$C_{m_q} = \frac{\partial C_m}{\partial \frac{\dot{\theta}\bar{c}}{2V}}$

$i = \sqrt{-1}$

D differential operator, $\frac{d}{dt}$

p La Place transform variable corresponding to differential operator

KG system or component transfer function; may be expressed as a function of $i\omega$, p, or D

DESCRIPTION OF THE PROPOSED CANARD MISSILE STABILIZATION AND CONTROL SYSTEM

The block diagram of the proposed system is shown in figure 1, and with the exception of the target seeker which responds to errors in attitude, or to command inputs θ_i, it is the same as the system of reference 1. The characteristics of the rate servo were obtained from reference 2, and the gain constant of the integrating servo K_2 was obtained from the Langley Pilotless Aircraft Research Division, based on the results presented in reference 1.

The missile used in this report is a symmetrical cruciform configuration as shown in figure 2. The wings and canard fins are of delta design with the leading edges swept back 60°. The estimated aerodynamic derivatives

and parameters of the over-all system as used in the calculations are given in table I.

METHOD OF ANALYSIS AND DISCUSSION

The purpose of this paper is to analyze the effect of time delay in the target-seeker response, and of various types of dead spots in the seeker on the longitudinal stability and response characteristics of the assumed missile.

The equations of motion for the system described in figure 1, assuming two degrees of freedom (α_o,θ_o), constant forward speed, and level flight for the airframe are:

$$\left.\begin{aligned}
&\left(\frac{I_Y}{qS\bar{c}} D^2 - C_{m_q} \frac{\bar{c}}{2V} D\right)\theta_o - \left(C_{m_\alpha} + C_{m_{\dot{\alpha}}} \frac{\bar{c}}{2V} D\right)\alpha_o = C_{m_\delta}\delta + C_m \\
&\frac{mV}{qS} D\theta_o - \left(\frac{mV}{qS} D + C_{L_\alpha}\right)\alpha_o = C_{L_\delta}\delta
\end{aligned}\right\} \quad (1)$$

where $\delta = \delta_s - \delta_R$. The quantities δ_s and δ_R are defined by the equations:

$$\delta_s = \frac{K_2}{D}(n_i - n_o) = K_2 \int_0^t (n_i - n_o)dt$$

$$\left(D^2 + 2\xi\omega_n D + \omega_n^2\right)\delta_R = K_r\omega_n^2 D\theta_o$$

and

$$(1 + \tau D)n_i = K_1\left(\theta_i - \theta_o\right)$$

The quantity n_o is the normal acceleration of the missile in terms of g, the acceleration due to gravity; that is:

$$n_o = \frac{V(D\theta_o - D\alpha_o)}{g}$$

If the substitutions be made that $D\alpha_o = D\theta_o - \frac{g}{V} n_o$ and $\alpha_o = \theta_o - \frac{g}{V}\frac{n_o}{D}$, the following equations in terms of θ_o and n_o result:

$$\left.\begin{aligned}
&\frac{I_Y}{qS\bar{c}} D^2\theta_o - \left(C_{m_q} + C_{m_{\dot{\alpha}}}\right)\frac{\bar{c}}{2V} D\theta_o - C_{m_\alpha}\theta_o + C_{m_{\dot{\alpha}}}\frac{g\bar{c}}{2V^2} n_o + \\
&\quad C_{m_\alpha}\frac{g}{V}\frac{n_o}{D} = C_{m_\delta}\delta + C_m \\
&\frac{W}{qS} n_o + C_{L_\alpha}\frac{g}{V}\frac{n_o}{D} - C_{L_\alpha}\theta_o = C_{L_\delta}\delta \\
&\delta = \delta_s - \delta_R \\
&\delta_s = K_2\int_0^t \left(n_i - n_o\right)dt \\
&\left(D^2 + 2\xi\omega_n D + \omega_n^2\right)\delta_R = K_r\omega_n^2 D\theta_o \\
&(1 + \tau D)n_i = K_1\left(\theta_i - \theta_o\right)
\end{aligned}\right\} \quad (1a)$$

For the flight condition of table I, these equations were solved by means of the Reeves Electronic Analog Computer for the transient responses θ_o, n_o, δ_s, δ, α_o, and γ_o subsequent to the input $\theta_i = 5^o$ or $C_m = 0.05$ which corresponds to a 5° control deflection. The C_m case corresponds to the application of a constant pitching moment, and the control system acts as a regulator which reduces the error signal $-\theta_o$ to zero in the steady-state condition.

Selection of target-seeker gain constant.- The first step in the analysis is to select a value of the target-seeker gain constant K_1 for which the system will have a satisfactory transient response to the inputs θ_i and C_m, hereinafter referred to as command and regulatory

responses, respectively. A criterion for the command response as suggested in reference 3 is that the closed-loop frequency response $\frac{\theta_o}{\theta_i}(i\omega)$ satisfy the condition:

$$\left|\frac{\theta_o}{\theta_i}(i\omega)\right|_{max} = 1.3$$

For the system of figure 1, $K_1 = 182$ satisfies this criterion. Transient responses were obtained from the Reeves Electronic Analog computer for a number of values of K_1 between 0 and 487 which is the value at which the system becomes unstable, for both θ_i and C_m inputs. Examination of these transients indicated that for $K_1 = 120$ the response characteristics of the system subsequent to the C_m input would be satisfactory, whereas for the θ_i input, $K_1 = 225$ appeared to be more nearly an optimum value for the seeker gain. Hence, for the analysis made to determine the effect of time delay and dead spot in the seeker on the transient response of the system, both values of K_1 were considered. In a subsequent section of the paper an explanation will be given as to why $K_1 = 225$ results in a better command response than does $K_1 = 182$. The factors considered in the selection of the target seeker gain were:

(1) Degree of stability

(2) Rise time (time to reach 95 percent of steady-state value)

(3) Response time (time to reach and remain within 95 percent of of steady-state value)

Since the primary purpose of the paper is to investigate the general effects of time delay and dead spot in the target seeker on the system response characteristics, no rigorous attempt was made to choose an optimum value for the target-seeker gain constant K_1, but rather, values were selected which gave generally satisfactory responses to the two types of inputs considered. Selection of the optimum value of K_1 would require manipulation of the gains of the other components of the system, particularly the gain of the pitch-rate feedback block, and the opinion was that the results of this investigation were not sufficiently dependent upon the choice of K_1 as to warrant such a detailed analysis.

Effect of time delay in target seeker.- The transfer function which defines the dynamic characteristics of the target seeker is assumed to be of the form

$$n_i(t) = \frac{K_1}{1 + \tau D} \epsilon_1(t) \tag{2}$$

For a step input $\epsilon_1(t) = \epsilon_1$, the response $n_i(t)$ is

$$n_i(t) = K_1\epsilon_1\left(1 - e^{\frac{-t}{\tau}}\right)$$

Thus, $n_i(t)$ approaches the value $K_1\epsilon_1$ exponentially, and the time required for $n_i(t)$ to reach any given percentage of its steady-state value varies directly with the quantity τ, which is referred to as the time constant of the system. Unpublished response data on the seeker indicated that the value of τ probably will not exceed 0.10. Transient responses subsequent to application of $C_m = 0.05$ and to the command input $\theta_i = 5^\circ$ for $\tau = 0$ and $\tau = 0.10$ are presented in figures 3 and 4 for $K_1 = 120$ and $K_1 = 225$. The general effect of increasing τ, as seen from these figures, is to make the responses somewhat less stable and to increase the period of the oscillation. In addition, the transients for $K_1 = 225$ are affected more by inclusion of this factor than are the ones for $K_1 = 120$. This is undoubtedly due to the fact that the system is considerably better damped for $K_1 = 120$ than for $K_1 = 225$; therefore, changes in stability are more easily detected for this latter value of K_1. Since the magnitude of the changes in the transients does not appear to be critical, and because the analysis is somewhat simplified by the assumption of $\tau = 0$, subsequent analysis made to determine the effect of dead spot in the seeker is based on this assumption. It is interesting to note that the missile normal acceleration n_o for the cases presented in figures 3 and 4 is well below the missile structural limit which has been estimated to be 30g. Also, as seen from these figures, the control deflections encountered should be relatively small.

The types of target-seeker nonlinearities considered in this analysis are illustrated in figure 5, and the equations which relate $n_i(t)$ and $\epsilon_1(t)$ for these cases are as follows:

Case I $\left.\right\}$ Linear case

or

$$n_i(t) = K_1\epsilon_1(t)$$

$$\text{Case II}\left\{\begin{array}{ll} n_i(t) = K_1\epsilon_1(t) & \left|\epsilon_1(t)\right| > \left(\epsilon_1\right)_o \\ n_i(t) = 0 & \left|\epsilon_1(t)\right| < \left(\epsilon_1\right)_o \end{array}\right.$$

$$\text{Case III}\left\{\begin{array}{ll} n_i(t) = K_1\left[\epsilon_1(t) + \left(\epsilon_1\right)_o\right] & \epsilon_1(t) < -\left(\epsilon_1\right)_o \\ n_i(t) = 0 & \left|\epsilon_1(t)\right| < \left(\epsilon_1\right)_o \\ n_i(t) = K_1\left[\epsilon_1(t) - \left(\epsilon_1\right)_o\right] & \epsilon_1(t) > \left(\epsilon_1\right)_o \end{array}\right.$$

$$\text{Case IV}\left\{\begin{array}{ll} n_i(t) = K_1\left[\epsilon_1(t) + \frac{\left(\epsilon_1\right)_o}{2}\right] & \epsilon_1(t) < -\left(\epsilon_1\right)_o \\ n_i(t) = \frac{K_1}{2}\,\epsilon_1(t) & \left|\epsilon_1(t)\right| < \left(\epsilon_1\right)_o \\ n_i(t) = K_1\left[\epsilon_1(t) - \frac{\left(\epsilon_1\right)_o}{2}\right] & \epsilon_1(t) > \left(\epsilon_1\right)_o \end{array}\right.$$

Transient responses for case I (linear case) are presented in figures 3 and 4. For case II transient responses were obtained for $K_1 = 120$ and $K_1 = 225$ for both θ_i and C_m inputs. The values of $\left(\epsilon_1\right)_o$ included in the analysis are $1/2^\circ$, 1°, $1\frac{1}{2}^\circ$, and 2°. For cases III and IV, only $K_1 = 225$ was considered and transients were obtained only for the θ_i input. The range of values of $\left(\epsilon_1\right)_o$ investigated was the same as for case II except that no results are presented for $\left(\epsilon_1\right)_o = 1\frac{1}{2}^\circ$.

The transients for case II are presented in figures 6 to 9. A comparison of the results of figures 8 and 9 with those of figure 4 indicates that, for the type of dead spot chosen as case II, the steady-state error ϵ_1 subsequent to the command input θ_i increases as the dead spot is increased and is essentially equal to the size of the dead spot. It should be noted that the step input to $n_i(t)$ as $\left|\epsilon_1\right| \rightarrow \left(\epsilon_1\right)_o$

is responsible for the apparent reexcitation of the transients which can be seen for $K_1 = 120$ (fig. 8). For the C_m or regulatory response, (figs. 6 and 7) the steady-state pitch error is seen to be smaller than for the command responses (figs. 8 and 9) for each value of $(\epsilon_1)_o$ and apparently independent of the value of $(\epsilon_1)_o$. This result can be attributed to the fact that whenever $|\epsilon_1| < (\epsilon_1)_o$ the target seeker is assumed to have no output; that is, $n_i(t) = 0$. When the target seeker is inoperative, it can be shown from the operational solution for $\theta_o(p)$, by use of the final value theorem $\left[\text{i.e., } \lim_{p \to 0} p\theta_o(p) = \lim_{t \to \infty} \theta_o(t)\right]$, that $\theta_o(t) \to 0$ subsequent to initial conditions, and $\theta_o(t)$ in degrees approaches the value $\frac{57.3C_m g}{C_{m_\delta} K_2 V}$ subsequent to initial conditions plus a constantly applied pitching-moment coefficient C_m. For the command-input case, the seeker becomes inoperative whenever $|\theta_i - \theta_o| < (\epsilon_1)_o$, and when the system is operating in this error range the tendency is to return toward $\theta_o = 0$. As the error again becomes larger than $(\epsilon_1)_o$, the target-seeker output is such as to cause the pitch error $|\theta_i - \theta_o|$ to be reduced. Thus, this procedure is continually repeated and, in the steady-state condition, $\theta_o = \theta_i - (\epsilon_1)_o$. For the response to an applied pitching moment C_m, the target seeker output signal is zero whenever $|\theta_o| < (\epsilon_1)_o$ (since $\theta_i = 0$). Thus, as was pointed out previously, the θ_o response when the system is operating within the dead spot tends toward the value $\frac{57.3C_m g}{C_{m_\delta} K_2 V}$, and when outside the dead spot the tendency is for the error to be reduced toward zero. It is apparent that if the magnitude of the dead spot is greater than the steady-state error for the system with the target seeker inoperative, the steady-state pitch error θ_o of the complete system must approach $\frac{57.3C_m g}{C_{m_\delta} K_2 V}$. For the cases discussed in this paper, this value is approximately 1°; since only one value of $(\epsilon_1)_o$ less than 1° is considered, the steady-state value of θ_o subsequent to $C_m = 0.05$ should be essentially independent of $(\epsilon_1)_o$, a result verified by the results of figures 6 and 7. As the dead spot is increased, the system is operating more and more in the error range where the target-seeker output is assumed to be zero and since this system is more stable when the target seeker is not operating there is an apparent increase in stability as $(\epsilon_1)_o$ is increased.

For the type of dead spot designated as case III, the only apparent effect on the command responses presented in figure 10 for $K_1 = 225$ is that the magnitude of the steady-state error in θ_o increases proportionally with increases in $(\epsilon_1)_o$. The frequency and damping of the transient motions are relatively unaffected by variations in $(\epsilon_1)_o$. Regulatory responses were not calculated for this case.

The command responses for $K_1 = 225$ obtained for the type of dead spot designated as case IV are presented in figure 11. The parameter, $K_1' = 113$ is the seeker gain when $|\epsilon_1| < (\epsilon_1)_o$. The steady-state error in θ_o is seen from figure 11 to be zero regardless of the value assumed for $(\epsilon_1)_o$. This result is to be expected since, for this type of dead spot, the seeker is sensitive to small errors as well as large, the only difference being that the seeker gain is not the same for small errors as for large errors. As $(\epsilon_1)_o$ increases, the responses tend to become more stable and the response time tends to increase. The cause for this increase in stability becomes apparent upon examination of the effect of seeker gain on the system stability which can be seen in figures 3 and 4. The system is seen to become less stable as K_1 is increased, and, since, as $(\epsilon_1)_o$ increases, the system is operating more and more in the error range where the seeker gain is K_1', the stability of the system is determined primarily by K_1'. For the case illustrated, $K_1' = 113$, which is close to the value of 120 discussed previously for K_1. Thus, as $(\epsilon_1)_o$ approaches 5° (since $\theta_i = 5^o$), the transient responses will approach those presented for $K_1 = 120$, $\theta_i = 5^o$. This conclusion is seen to be correct from a comparison of the command responses for $K_1 = 120$ of figure 8 and the command response for $(\epsilon_1)_o = 2^o$ presented in figure 11(c) for which $K_1 = 225$ and $K_1' = 113$. No regulatory responses were calculated for this case.

Effect of considering the dynamic characteristics of the rate-sensitive autopilot.- The transfer function of the autopilot sensitive to rate of pitch is seen from the equations of motion to be

$$\frac{\delta_R}{\theta_o} = \frac{K_r \omega_n^2 D}{D^2 + 2\xi\omega_n D + \omega_n^2} \tag{3}$$

Often, as a simplification, rate autopilots are assumed to have ideal characteristics, that is, no variation of gain with frequency, and zero phase shift at all frequencies. The equation which relates δ_R and θ_o, when this assumption is made, is

$$\delta_R = K_r D\theta_o$$

Thus, approximation of the rate block by this equation results simply in the introduction of an increment to the stability derivative C_{m_q} in the amount:

$$\Delta C_{m_q} = C_{m_\delta} K_r \frac{2V}{\bar{c}}$$

Since the natural frequency and damping ratio were thought to be high enough to warrant this assumption, additional calculations were made to determine the target-seeker gain constant K_1 for which the system would become unstable when this simplification is introduced and it was found to be approximately 315. As was pointed out previously, when the dynamics of the rate block were included, the value of K_1 for which the system became unstable was 487. For purposes of comparison, transient motions subsequent to the input $\theta_i = 5^\circ$ were calculated for $K_1 = 300$ for both cases and the results are presented in figure 12. As was predicted by these calculations, the motion is considerably less stable for the idealized case than for the case where the autopilot dynamics were considered. This condition is in agreement with the results of a theoretical method (as yet unpublished) by the authors of the present paper which indicate that for certain combinations of ξ and ω_n it is possible for an autopilot characterized by a second-order differential equation to be a more effective means of stabilization than an idealized one for which the same static sensitivity is assumed.

Effect of seeker gain and time delay on the closed-loop frequency response, $\frac{\theta_o}{\theta_i}(i\omega)$.- The system closed-loop frequency response $\frac{\theta_o}{\theta_i}(i\omega)$, which can be derived from the block diagram of figure 1, is of the form:

$$\frac{\theta_o}{\theta_i}(i\omega) = \frac{\frac{\theta_o}{\epsilon_1}(i\omega)}{1 + \frac{\theta_o}{\epsilon_1}(i\omega)} \tag{4}$$

where $\frac{\theta_o}{\epsilon_1}(i\omega)$ is referred to as the open-loop frequency response. The function $\frac{\theta_o}{\epsilon_1}(i\omega)$, in terms of the transfer functions of the various components of the system, is

$$\frac{\theta_o}{\epsilon_1}(i\omega) = \frac{\left(\frac{\theta_o}{\delta}\right)\left(\frac{\delta_s}{\epsilon_2}\right)\left(\frac{n_i}{\epsilon_1}\right)}{1 + \left(\frac{\theta_o}{\delta}\right)\left[\left(\frac{\delta_s}{\epsilon_2}\right)\left(\frac{n_o}{\theta_o}\right) + \left(\frac{\delta_R}{\theta_o}\right)\right]} = x(\omega) + iy(\omega) \tag{5}$$

The component transfer functions for the data given in table I are

$$\frac{\theta_o}{\delta}(i\omega) = \frac{363.4(2.63 + i\omega)}{-6.30\omega^2 + i\omega(393 + \omega^2)} = K_3G_3$$

$$\frac{\delta_s}{\epsilon_2}(i\omega) = \frac{-0.067i}{\omega} = K_2G_2$$

$$\frac{n_i}{\epsilon_1}(i\omega) = \frac{K_1}{1 + i\tau\omega} = K_1G_1$$

$$\frac{n_o}{\theta_o}(i\omega) = \frac{169.4i\omega}{2.63 + i\omega} = K_5G_5$$

$$\frac{\delta_R}{\theta_o}(i\omega) = \frac{518i\omega}{(7744 - \omega^2) + 88i\omega} = K_4G_4$$

Open-loop frequency response plots in the (x,y) plane for $K_1 = 120$, 182, and 225 are presented in figure 13 for $\tau = 0$. For $K_1 = 225$ the plot for $\tau = 0.10$ is also presented. The value $K_1 = 182$ was included since this value results in a maximum value of $\left|\frac{\theta_o}{\theta_i}(i\omega)\right|$ equal to 1.3, the criterion suggested in reference 3. It is interesting to note that

the value $K_1 = 225$ which was used for the bulk of the analysis, on the basis of computed transients, does not differ greatly from the gain obtained by applying the criterion of reference 3.

The closed-loop frequency response plots for $K_1 = 120$, 182, and 225 are presented in figure 14 for $\tau = 0$. The plots presented are $\left|\frac{\theta_o}{\theta_i}\right|$ against frequency and the phase angle of $\frac{\theta_o}{\theta_i}$ against frequency. The maximum value of $\left|\frac{\theta_o}{\theta_i}\right|$ for $K_1 = 225$ is about 1.75, which is somewhat higher than the value 1.3 obtained for $K_1 = 182$. The plots of $\left|\frac{\theta_o}{\theta_i}\right|$ for each value of K_1 are seen from figure 14 to have a "bucket" at frequencies less than the natural frequency of the system, and, in addition, the curves drop off toward zero rather rapidly for frequencies greater than the natural frequency. This bucket at the low frequencies is due primarily to the characteristics of the airframe transfer function $\frac{n_o}{\delta}(i\omega)$, and by proper manipulation of the integrating-servo gain and the rate feedback gain, this condition could be considerably improved. As was pointed out previously, the opinion was that the results of this investigation were not sufficiently dependent upon the selection of optimum gains to warrant such a detailed analysis. The general effect of these characteristics on the output transient subsequent to a command input θ_i can be seen from examination of the expression for θ_o in terms of the closed-loop frequency response, which is

$$\theta_o(t) = \frac{(AR)_{\omega=0}}{2} + \frac{2}{\pi}\sum_{k=1}^{\infty}\frac{(AR)_{\omega_k}}{k}\sin\left[k\omega_o t + (PA)_{\omega_k}\right] \tag{6}$$

$$(k = 1, 3, 5, \ldots)$$

The terms $(AR)_{\omega_k}$ and $(PA)_{\omega_k}$ refer to the values of the amplitude ratio $\left|\frac{\theta_o}{\theta_i}\right|$ and the phase angle of $\frac{\theta_o}{\theta_i}$ at $\omega = k\omega_o$, respectively, where ω_o is the frequency of the square wave input θ_i. If $(AR)_{\omega_k} = 1$ and $(PA)_{\omega_k} = 0$ for all frequencies, then equation (6) becomes the Fourier series for the square wave. Thus, if these conditions existed, the system output would be identical with the input, and its response would be a perfect one. The attenuation of the low-frequency components

of the motion, as indicated by the so-called bucket at the low frequencies, tends to increase the time required for the output to reach and remain within a given percentage of its steady-state value, and the rapid reduction in $(AR)_{\omega_k}$ for frequencies beyond the system natural frequency effectively reduces the slope of the output curve immediately subsequent to $t = 0$. This latter effect can be seen from differentiation of equation (6) and noting that the high-frequency terms, for small values of t, are more important in this resulting expression than they are in equation (6). Also, the initial peak in the output is reduced by both of these characteristics. Thus, an analysis of the closed-loop frequency response plots for $K_1 = 182$ and $K_1 = 225$ would have indicated that the response for $K_1 = 225$ is slightly superior to that for $K_1 = 182$ since the higher value for $\left|\frac{\theta_o}{\theta_i}(i\omega)\right|_{max}$ when $K_1 = 225$ tends to compensate somewhat for the attenuation of the low-frequency inputs and decreases the system response time, as well as increasing the initial peak in the output. This is the same general result as was obtained from analysis of the computed transients.

The closed-loop plot for $\tau = 0.10$, and $K_1 = 225$ is also presented in figure 14, and since $\left|\frac{\theta_o}{\theta_i}\right|_{max}$ is considerably higher than for $\tau = 0$ and the bucket is not as deep, it is to be expected that the output would approach its steady-state value a little faster, and in addition have a higher initial peak which indicates a reduction in the system stability. The attenuation of the higher frequencies is greater than for $\tau = 0$ and hence the initial slope of the output plot is less for $\tau = 0.10$ than for $\tau = 0$. Also, this closed-loop plot clearly indicates a decrease in the natural frequency of the system. Thus, as for $\tau = 0$, the closed-loop plot for $\tau = 0.10$ indicates the same general trends as were obtained from the computed transients.

CONCLUSIONS

The following conclusions were reached from a theoretical investigation of the dynamic longitudinal performance characteristics of an automatically stabilized canard missile configuration equipped with an attitude-sensitive target seeker:

1. From an analysis of the missile motions for various values of target-seeker gain constant K_1, a value of K_1 may be selected for which the system has satisfactory stability and response characteristics.

2. The effect of time delay in the seeker is to decrease the system stability and to increase the period of the missile longitudinal oscillation. Also the missile response time tends to be increased. However, for the range of time constants investigated, these effects were not large.

3. The most significant effect of dead spot in the target seeker is to introduce a steady-state pitch error subsequent to command inputs. The magnitude of the steady-state error increases with increases in dead spot and is essentially equal to the magnitude of the dead spot.

4. For the type of nonlinearity in the seeker which results in a different gain for small errors than for large errors, the general effect is for the system to appear to have different stability and response characteristics for different error magnitudes. No steady-state error is introduced for this case and the stability of the system as it approaches a steady-state condition is determined primarily by the seeker gain which exists for small errors.

5. The stability of the investigated missile system was found to be much higher when the pitch-rate sensitive stabilization system was assumed to be characterized by a second-order linear differential equation rather than by an idealized system without phase lag.

6. Frequency-response analysis was useful in selecting the system gain and afforded a means of qualitatively estimating the effect of gain and time delay on the missile transient responses.

Langley Aeronautical Laboratory
National Advisory Committee for Aeronautics
Langley Field, Va.

REFERENCES

1. Seaberg, Ernest C., and Smith, Earl F.: Theoretical Investigation of an Automatic Control System with Primary Sensitivity to Normal Accelerations as Used to Control a Supersonic Canard Missile Configuration. NACA RM L51D23, 1951.

2. Nelson, Walter C., and Passera, Anthony L.: A Theoretical Investigation of the Influence of Auxiliary Damping in Pitch on the Dynamic Characteristics of a Proportionally Controlled Supersonic Canard Missile Configuration. NACA RM L50F30, 1950.

3. Brown, Gordon S., and Campbell, Donald P.: Principles of Servomechanisms. John Wiley & Sons, Inc., 1948.

TABLE I

ESTIMATED MASS AND AERODYNAMIC CHARACTERISTICS OF THE MISSILE

CONFIGURATION AND CONTROL SYSTEM PARAMETERS

I_Y, slug/ft^2	31.3
m, slugs	5.05
S, sq ft	4.1
$\bar{c}$, ft	1.776
C_{m_α}, per radian	-0.613
C_{L_α}, per radian	2.46
C_{m_q}, per radian/sec	-6.39
$C_{m_{\dot{\alpha}}}$, per radian/sec	-0.717
C_{m_δ}, per radian	0.573
C_{L_δ}, per radian	0
K_2, radians/sec/g	0.067
K_r, radians/rad/sec	0.067
ξ	0.50
ω_n, radians/sec	88
V, ft/sec	2074
Mach number	2.0
Altitude, ft	20,000
q, lb/sq ft	2725

NACA

CONFIDENTIAL

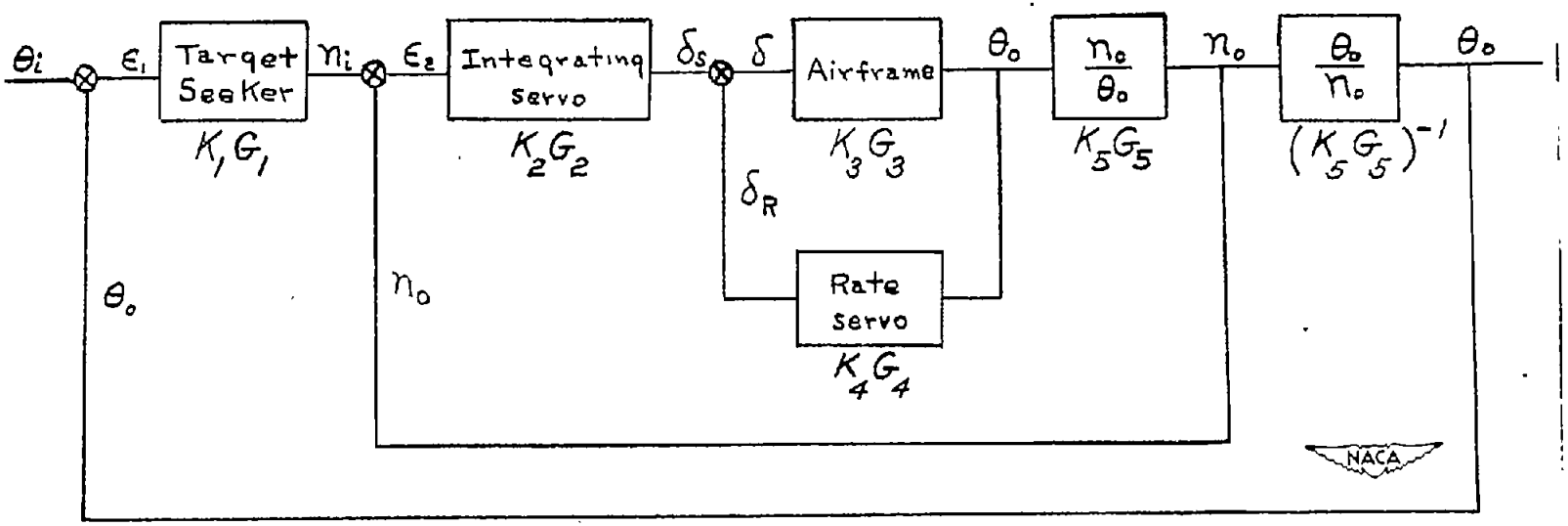

Figure 1.- Block diagram of the proposed missile control system.

CONFIDENTIAL

CONFIDENTIAL

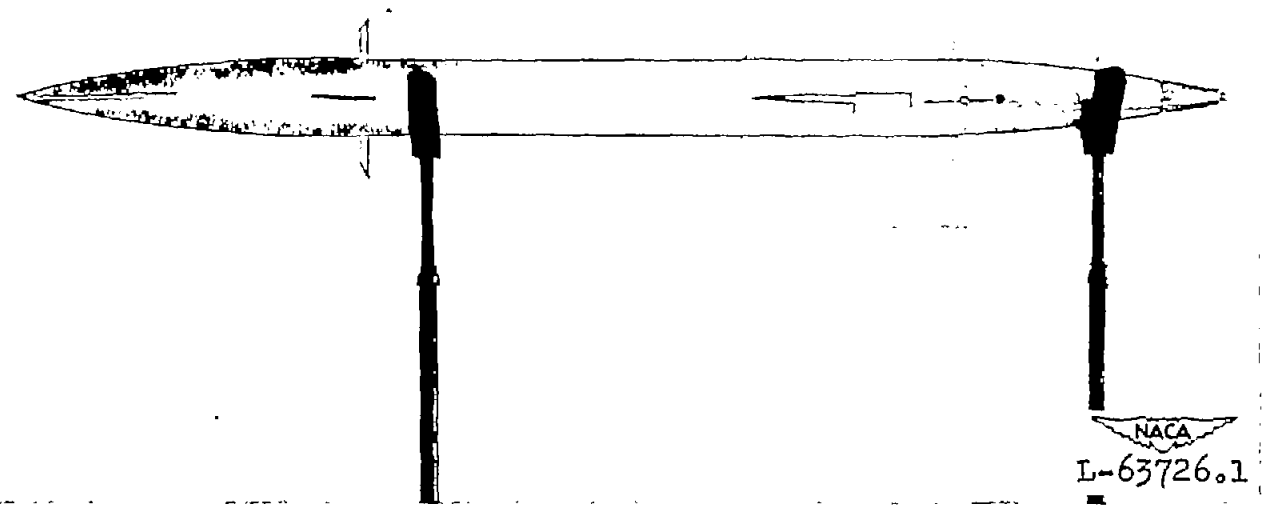

Figure 2.- Supersonic missile research model.

CONFIDENTIAL

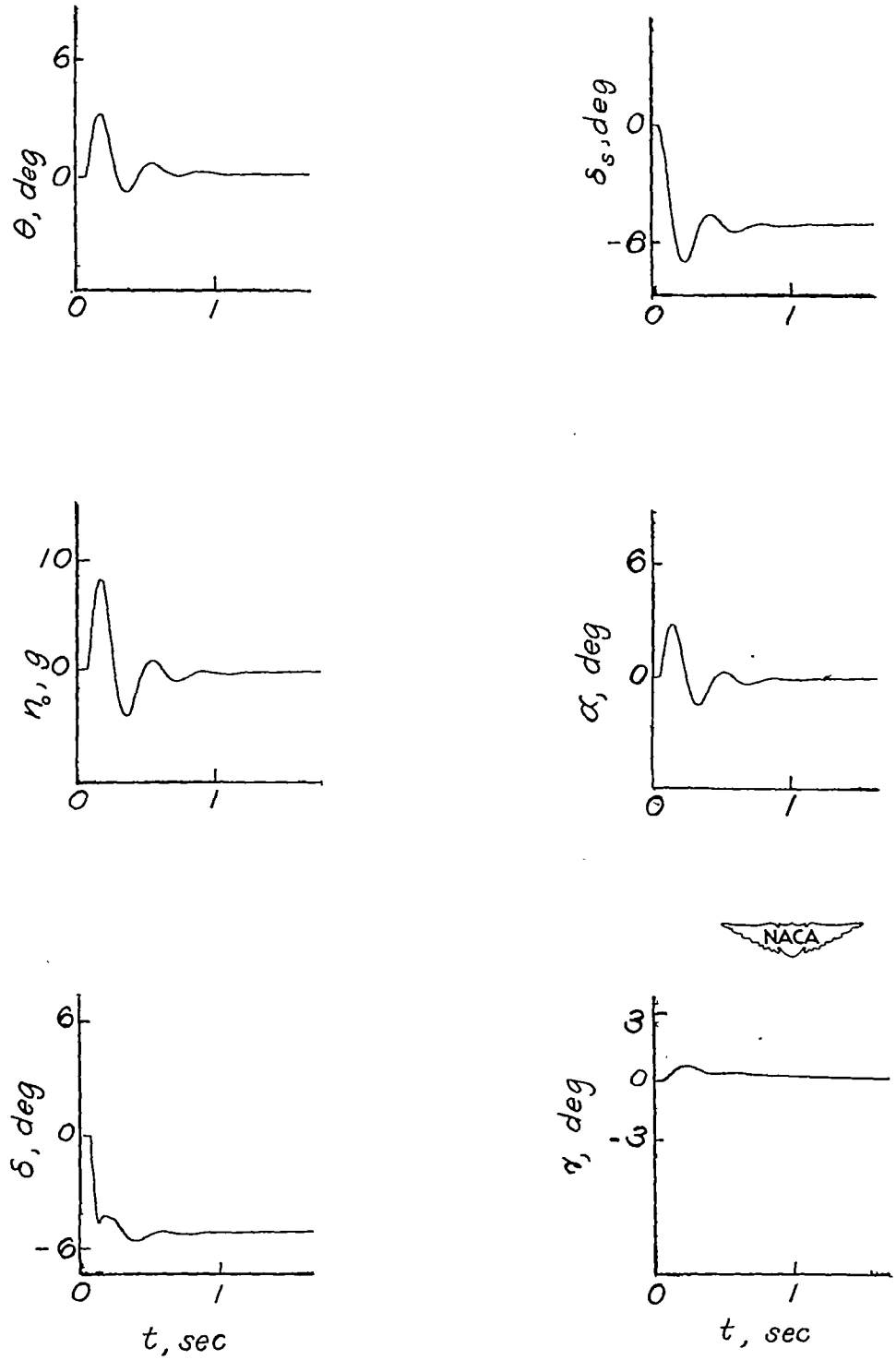

(a) $K_1 = 120$; $\tau = 0$.

Figure 3.- Calculated missile longitudinal responses subsequent to application of pitching-moment coefficient $C_m = 0.05$.

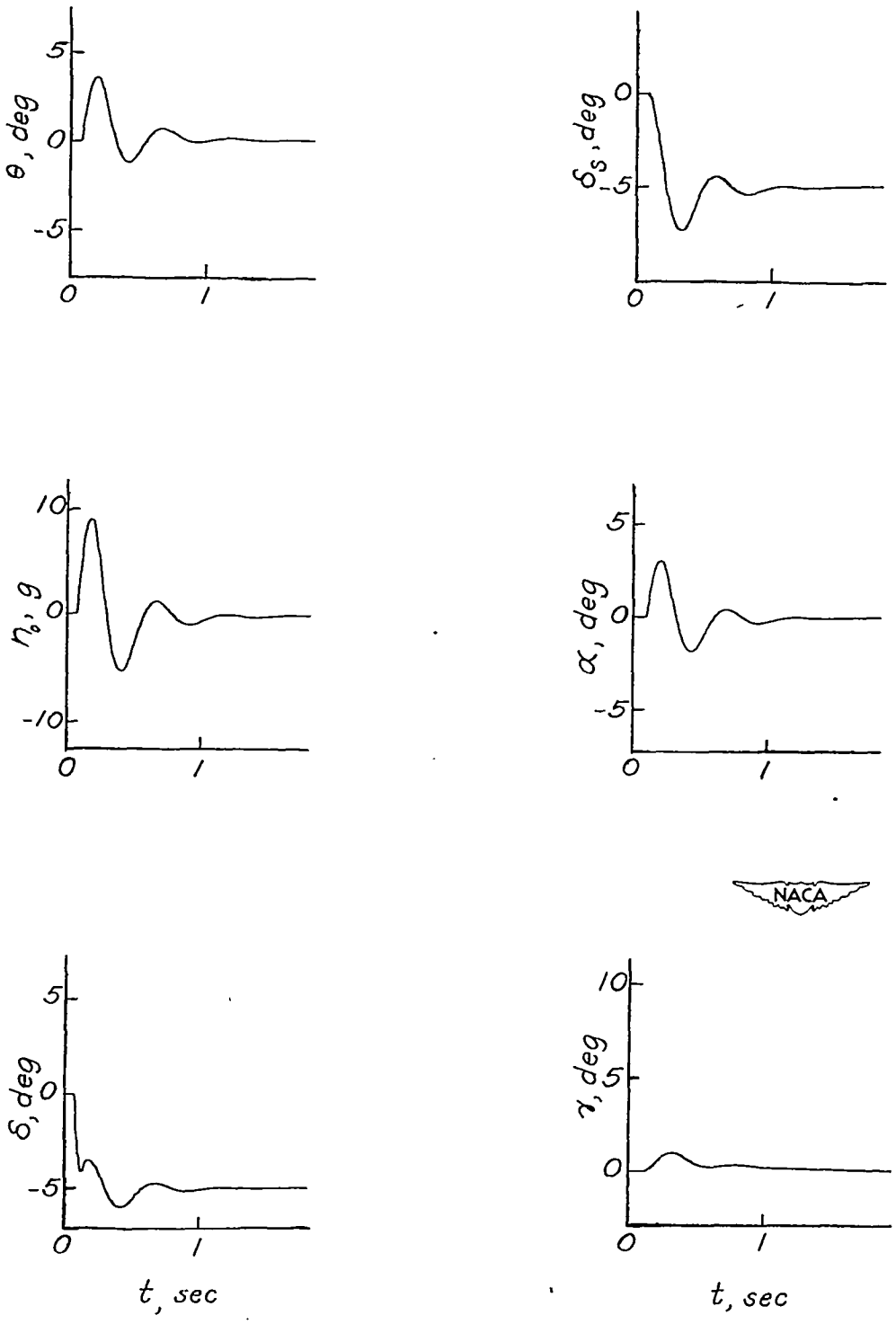

(b) $K_1 = 120$; $\tau = 0.10$.

Figure 3.- Continued.

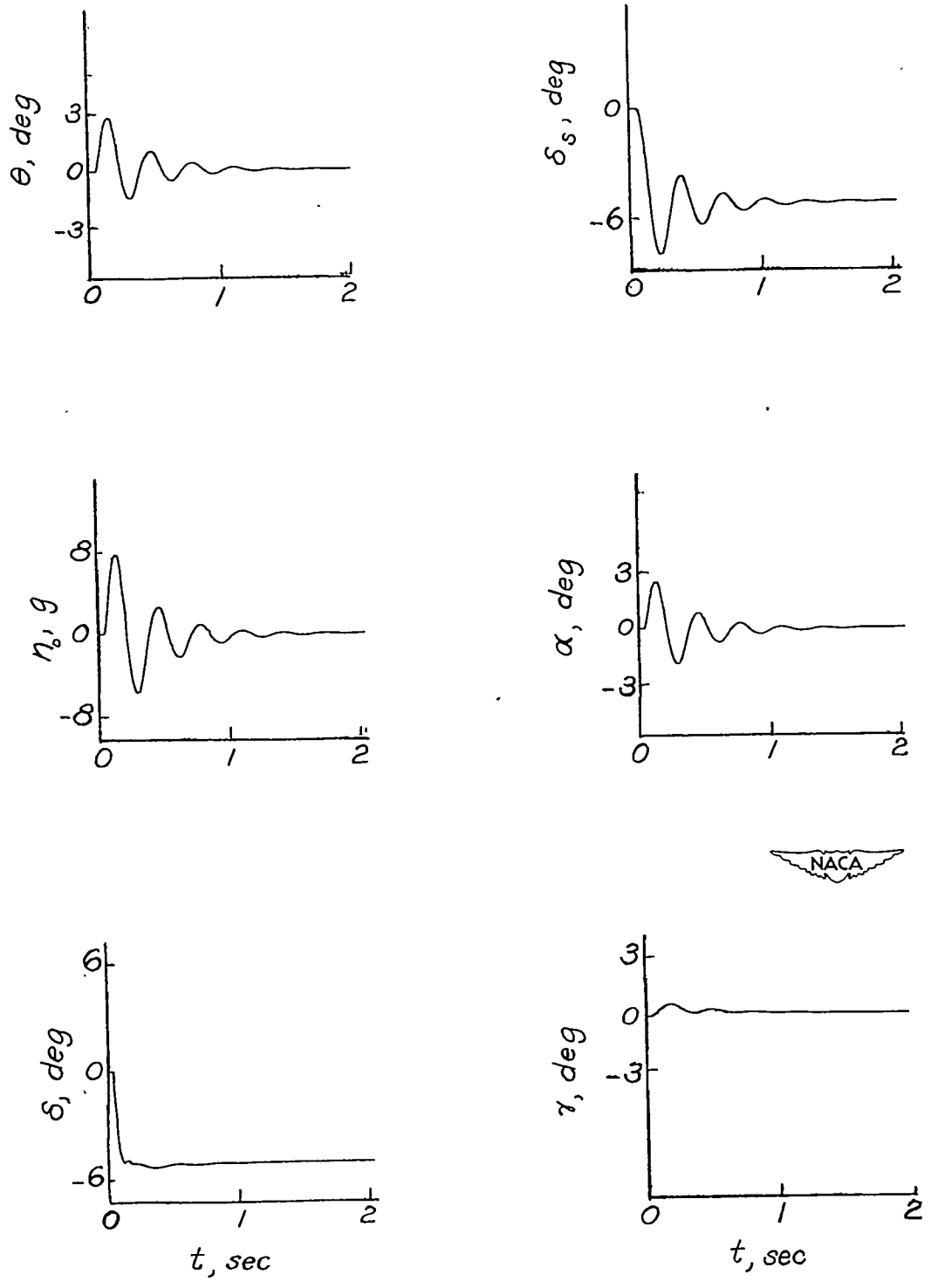

(c) $K_1 = 225$; $\tau = 0$.

Figure 3.- Continued.

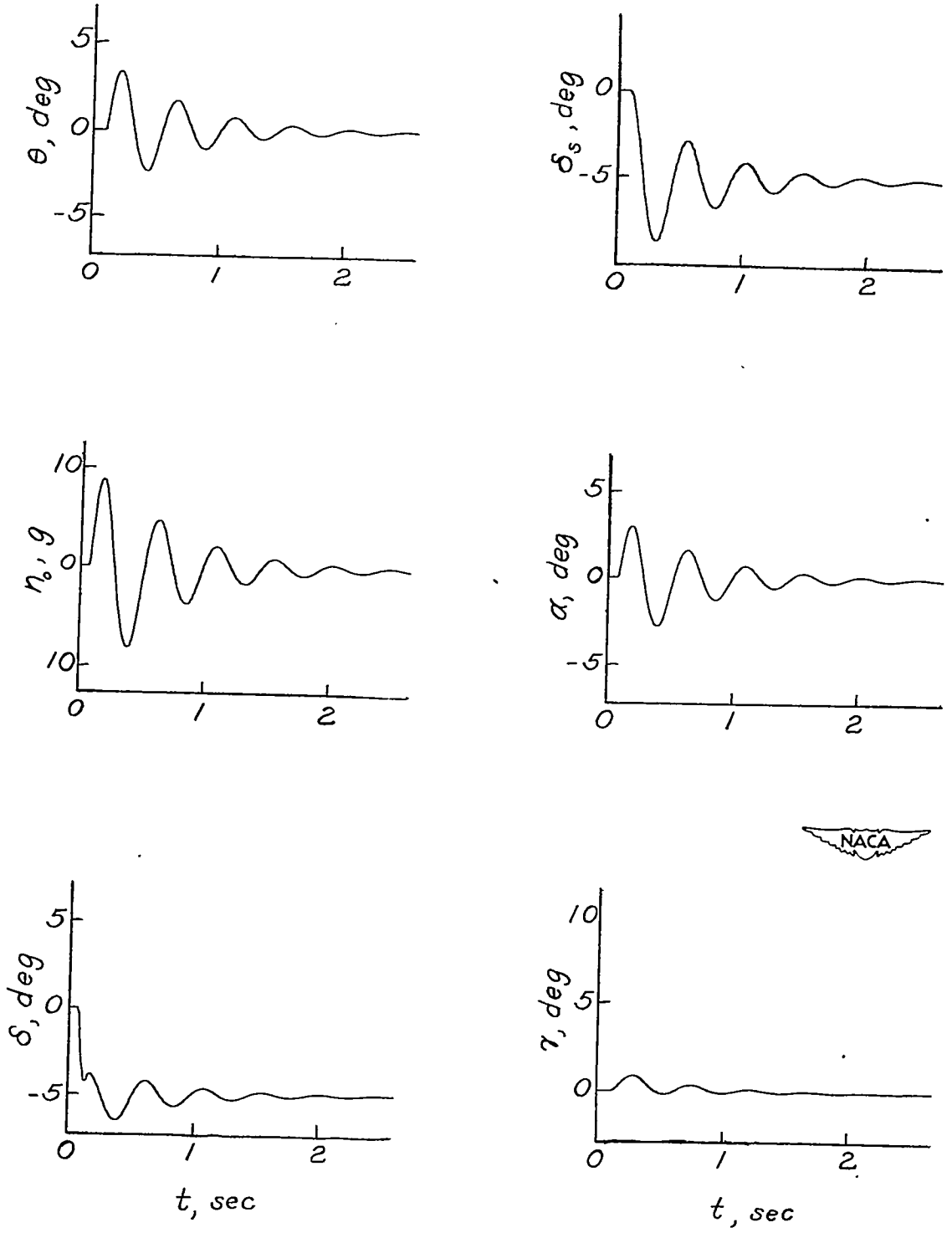

(d) $K_1 = 225$; $\tau = 0.10$.

Figure 3.- Concluded.

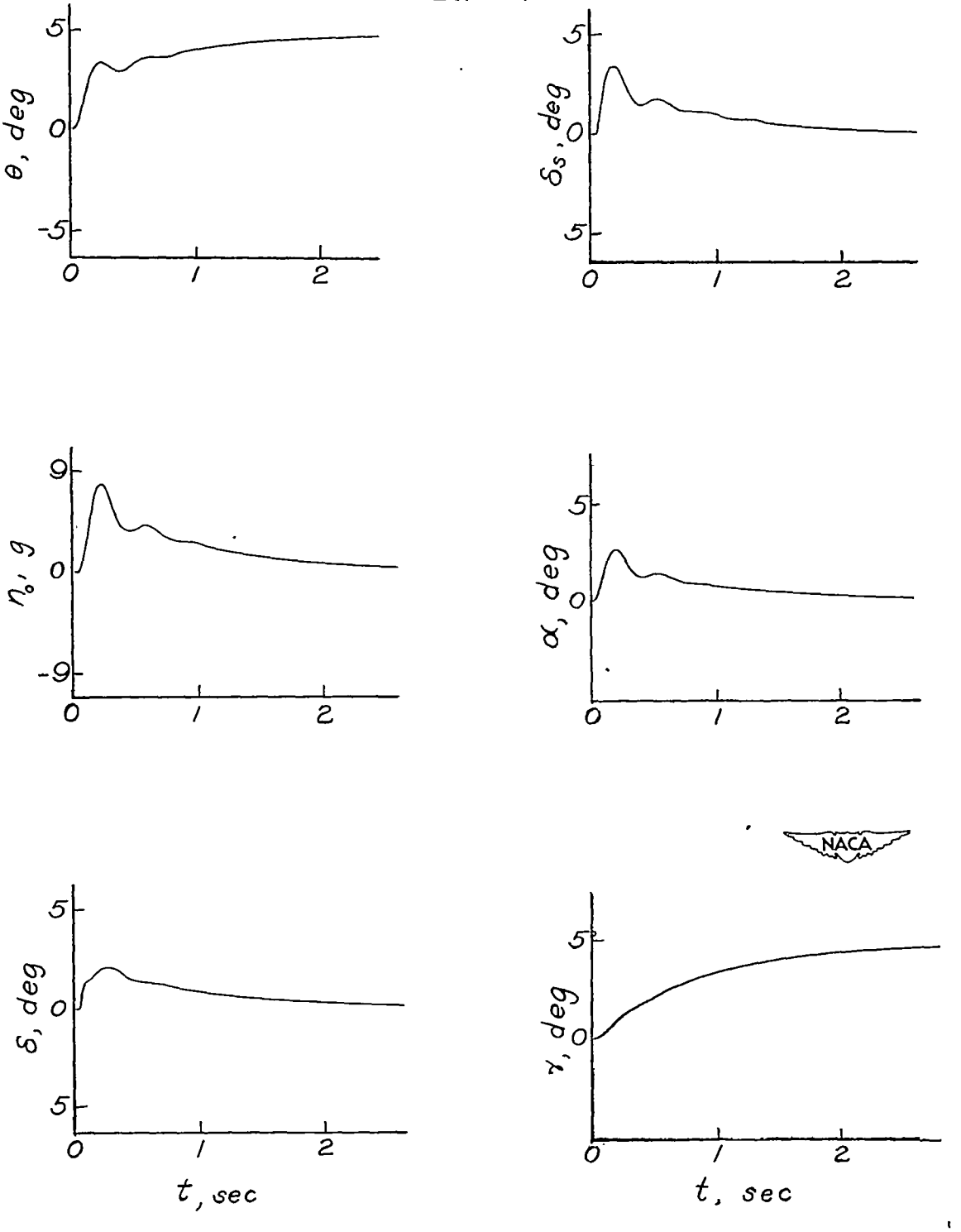

(a) $K_1 = 120$; $\tau = 0$.

Figure 4.- Calculated missile longitudinal responses subsequent to the command input $\theta_i = 5^{\circ}$.

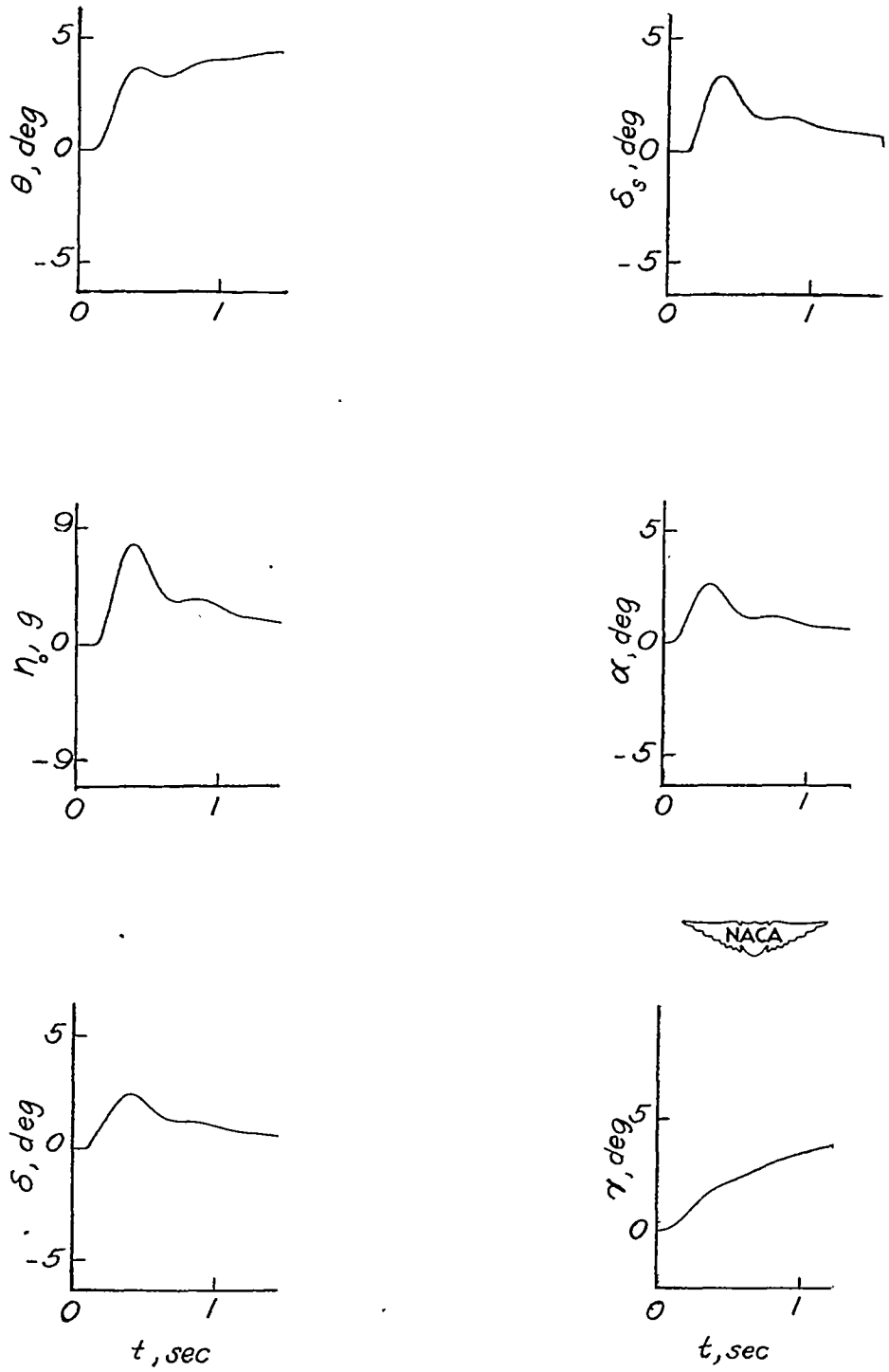

(b) $K_1 = 120$; $\tau = 0.10$.

Figure 4.- Continued.

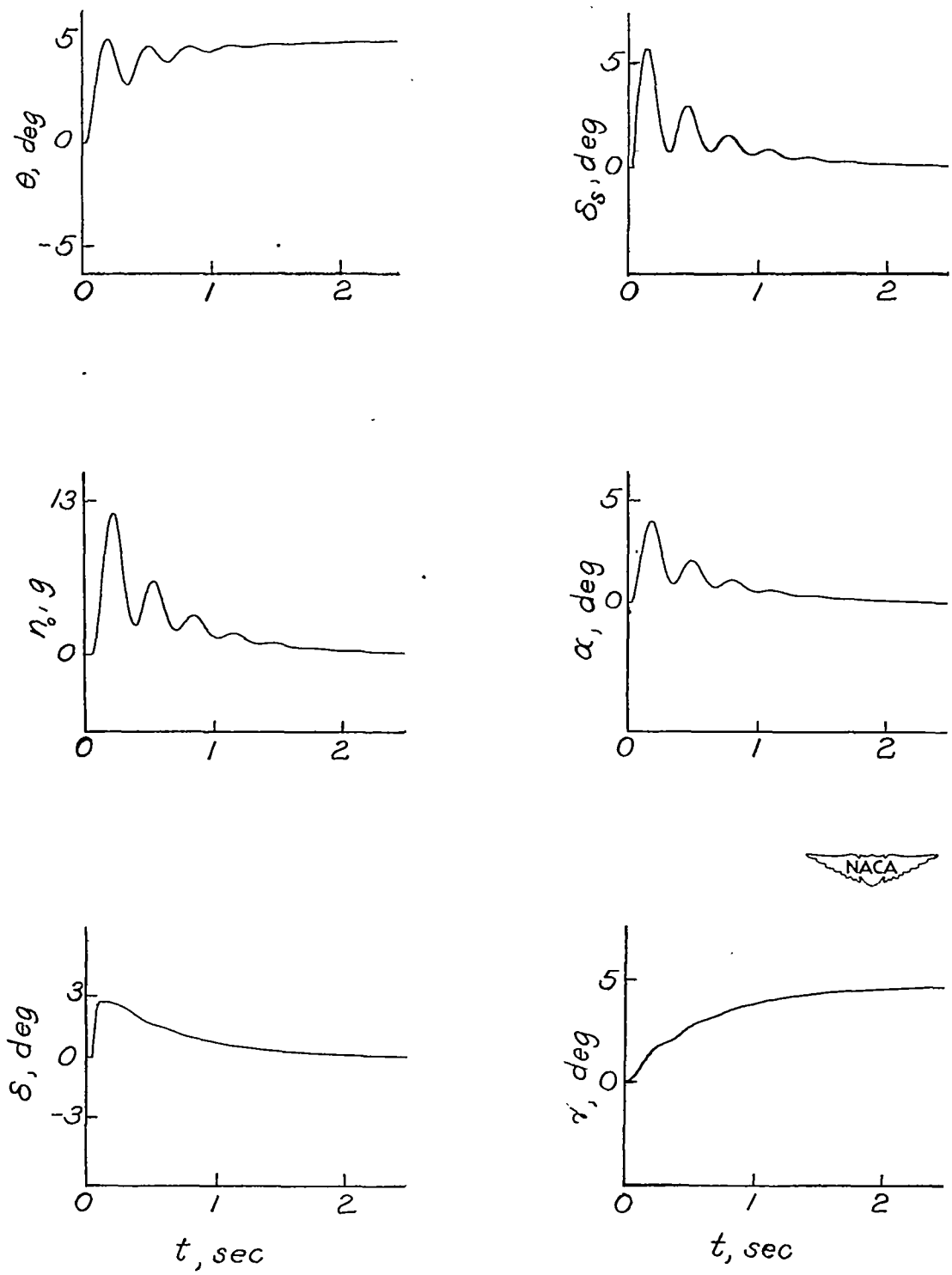

(c) $K_1 = 225$; $\tau = 0$.

Figure 4.- Continued.

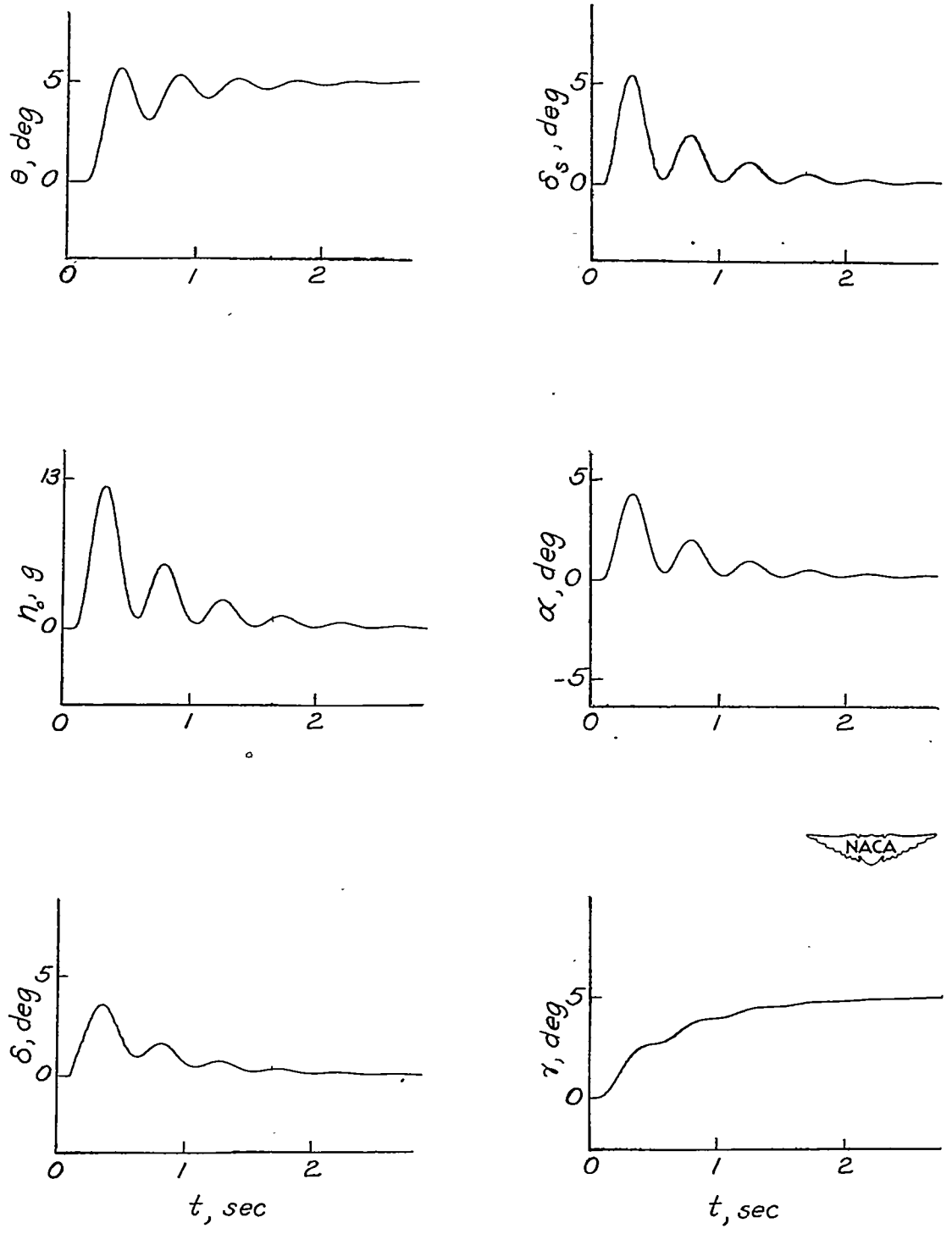

(d) $K_1 = 225$; $\tau = 0.10$.

Figure 4.- Concluded.

CONFIDENTIAL

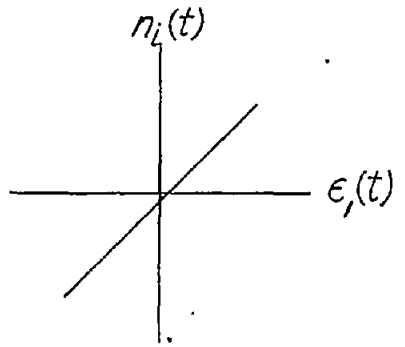

(a) Case I.

$n_i(t) = K_1\epsilon_1(t)$

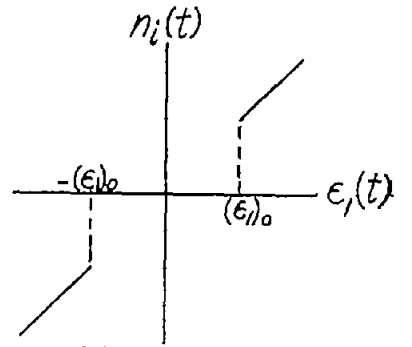

(b) Case II.

$n_i(t) = K_1\epsilon_1(t) \qquad |\epsilon_1(t)| > (\epsilon_1)_o$

$n_i(t) = 0 \qquad |\epsilon_1(t)| < (\epsilon_1)_o$

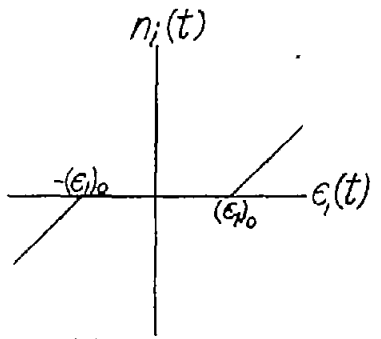

(c) Case III.

$n_i(t) = K_1\left[\epsilon_1(t) + (\epsilon_1)_o\right] \qquad \epsilon_1(t) < -(\epsilon_1)_o$

$n_i(t) = 0 \qquad |\epsilon_1(t)| < (\epsilon_1)_o$

$n_i(t) = K_1\left[\epsilon_1(t) - (\epsilon_1)_o\right] \qquad \epsilon_1(t) > (\epsilon_1)_o$

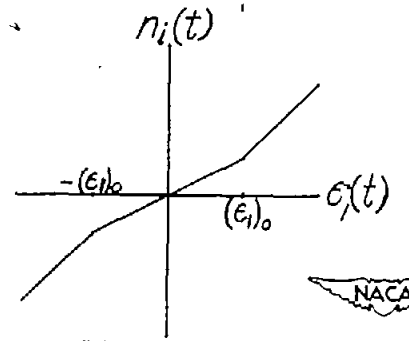

(d) Case IV.

$n_i(t) = K_1\left[\epsilon_1(t) + \frac{(\epsilon_1)_o}{2}\right] \qquad \epsilon_1(t) < -(\epsilon_1)_o$

$n_i(t) = \frac{K_1}{2}\epsilon_1(t) \qquad |\epsilon_1(t)| < (\epsilon_1)_o$

$n_i(t) = K_1\left[\epsilon_1(t) - \frac{(\epsilon_1)_o}{2}\right] \qquad \epsilon_1(t) > (\epsilon_1)_o$

Figure 5.- Types of target-seeker nonlinearities considered in analysis.

CONFIDENTIAL

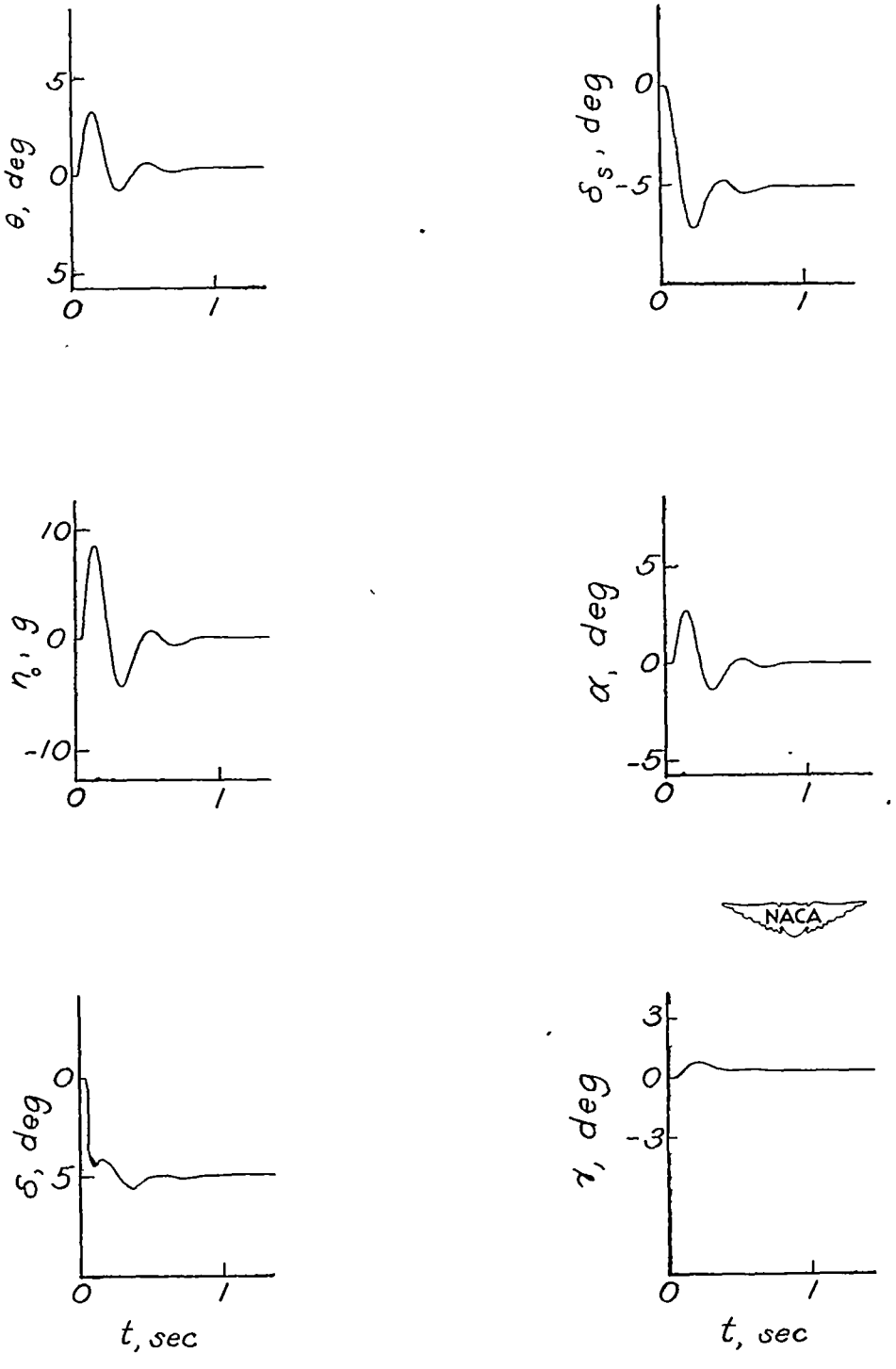

(a) Dead spot equal to 1/2°.

Figure 6.- Effect of dead spot, case II, on missile longitudinal responses subsequent to $C_m = 0.05$. $K_1 = 120$.

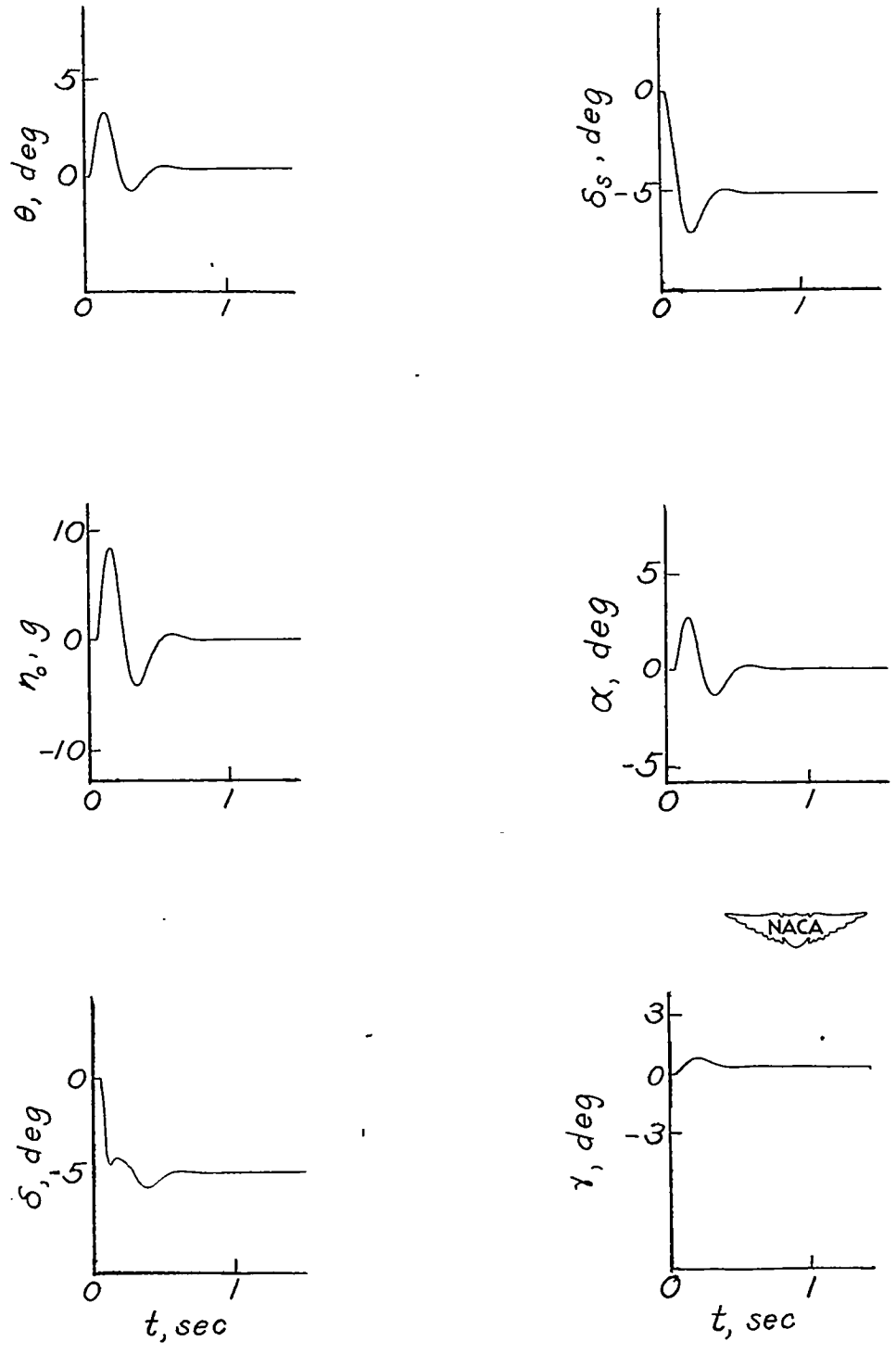

(b) Dead spot equal to 1°.

Figure 6.- Continued.

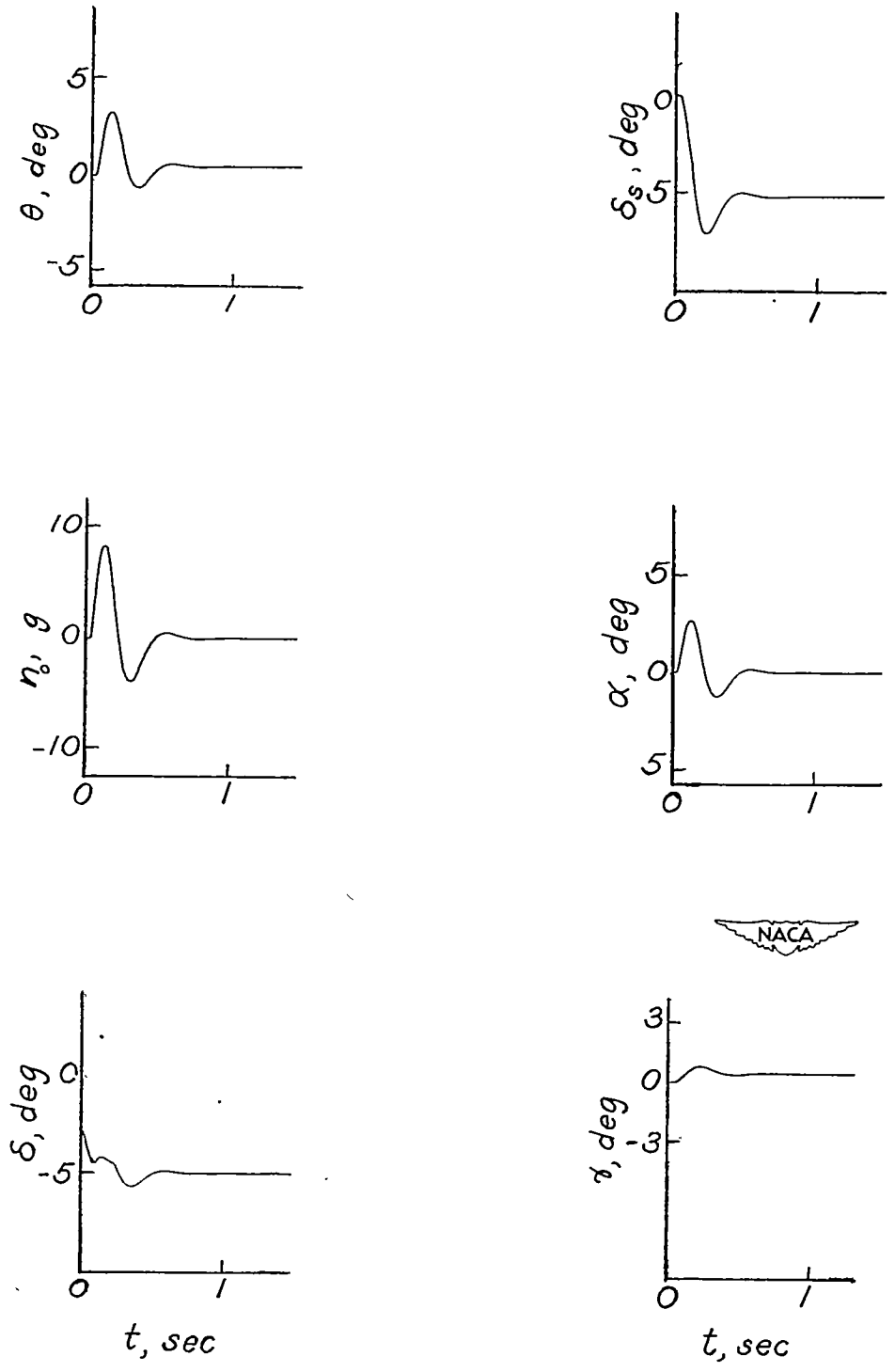

(c) Dead spot equal to $1\frac{1}{2}^{\circ}$.

Figure 6.- Continued.

5H

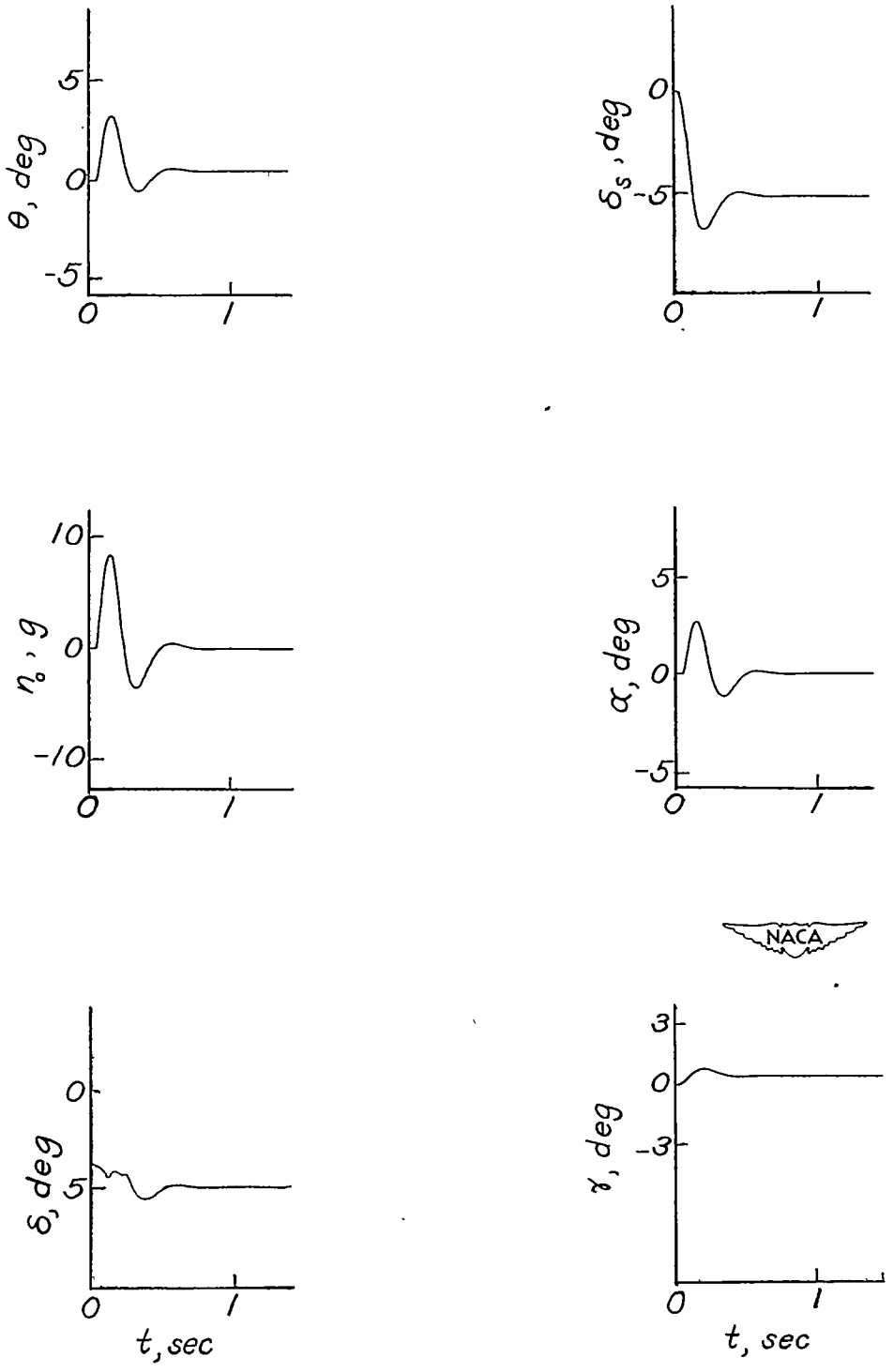

(d) Dead spot equal to 2°.

Figure 6.- Concluded.

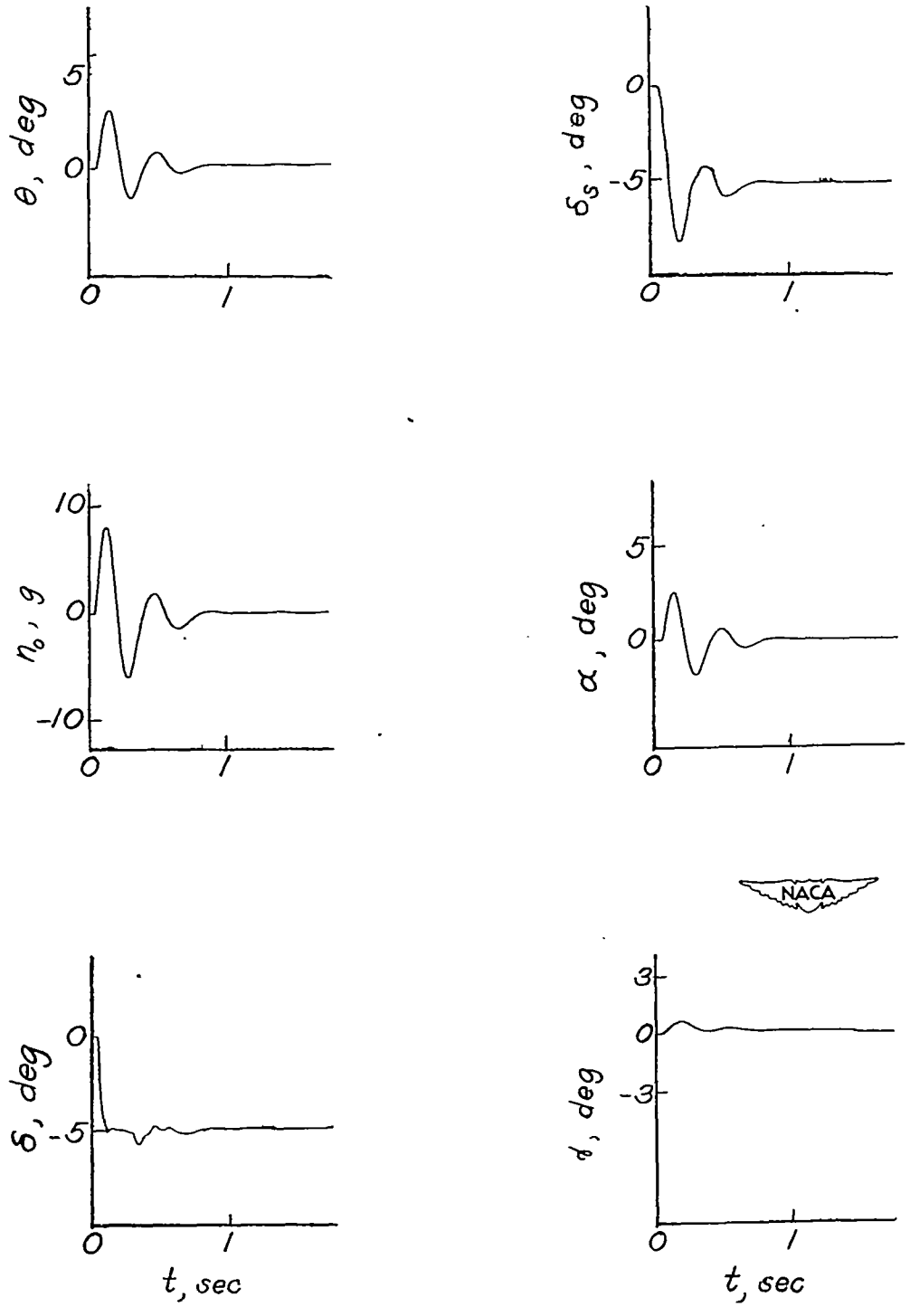

(a) Dead spot equal to 1/2°.

Figure 7.- Effect of dead spot, case II, on missile longitudinal responses subsequent to $C_m = 0.05$. $K_1 = 225$.

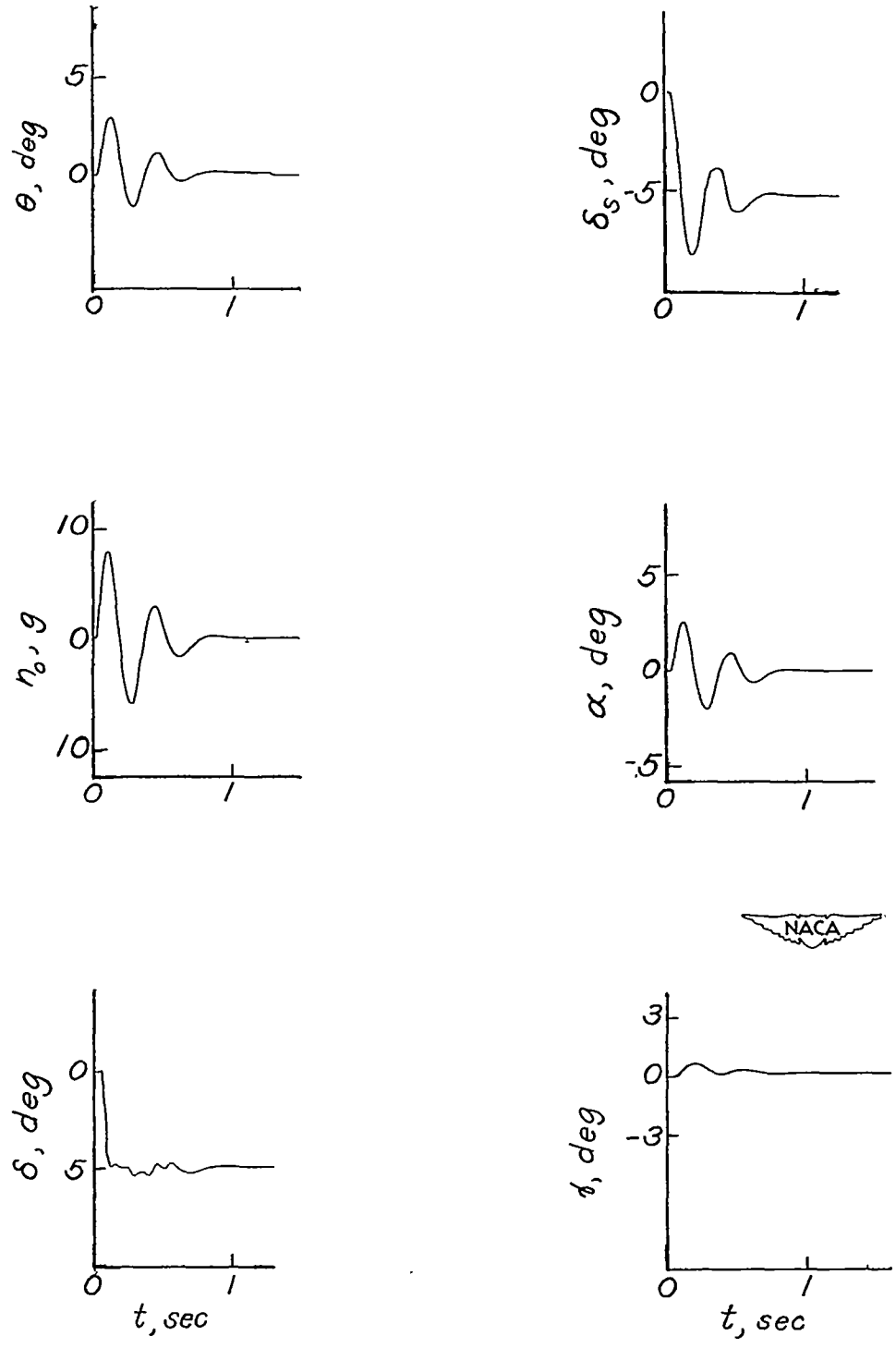

(b) Dead spot equal to 1°.

Figure 7.- Continued.

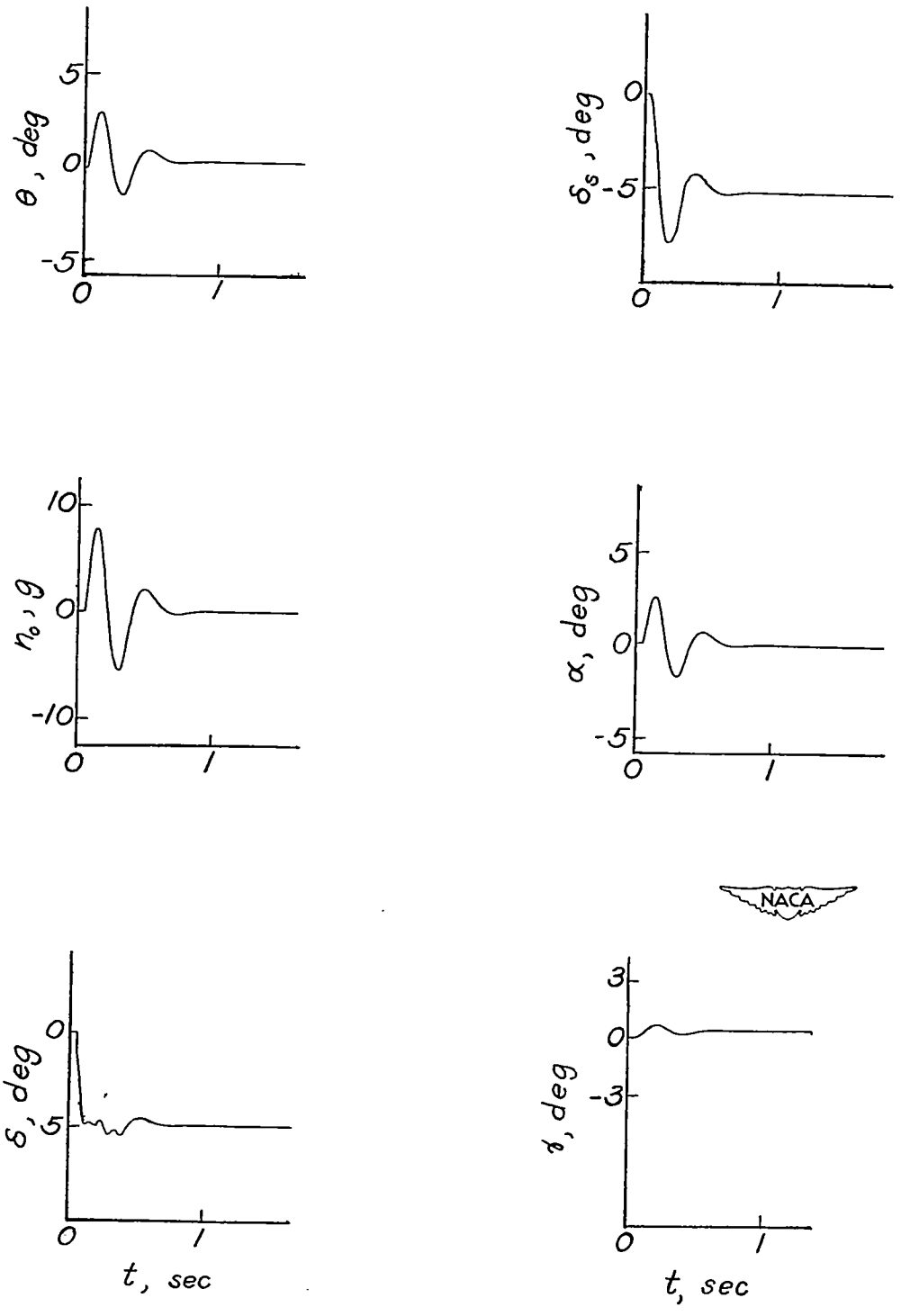

(c) Dead spot equal to $1\frac{1}{2}^{\circ}$.

Figure 7.- Continued.

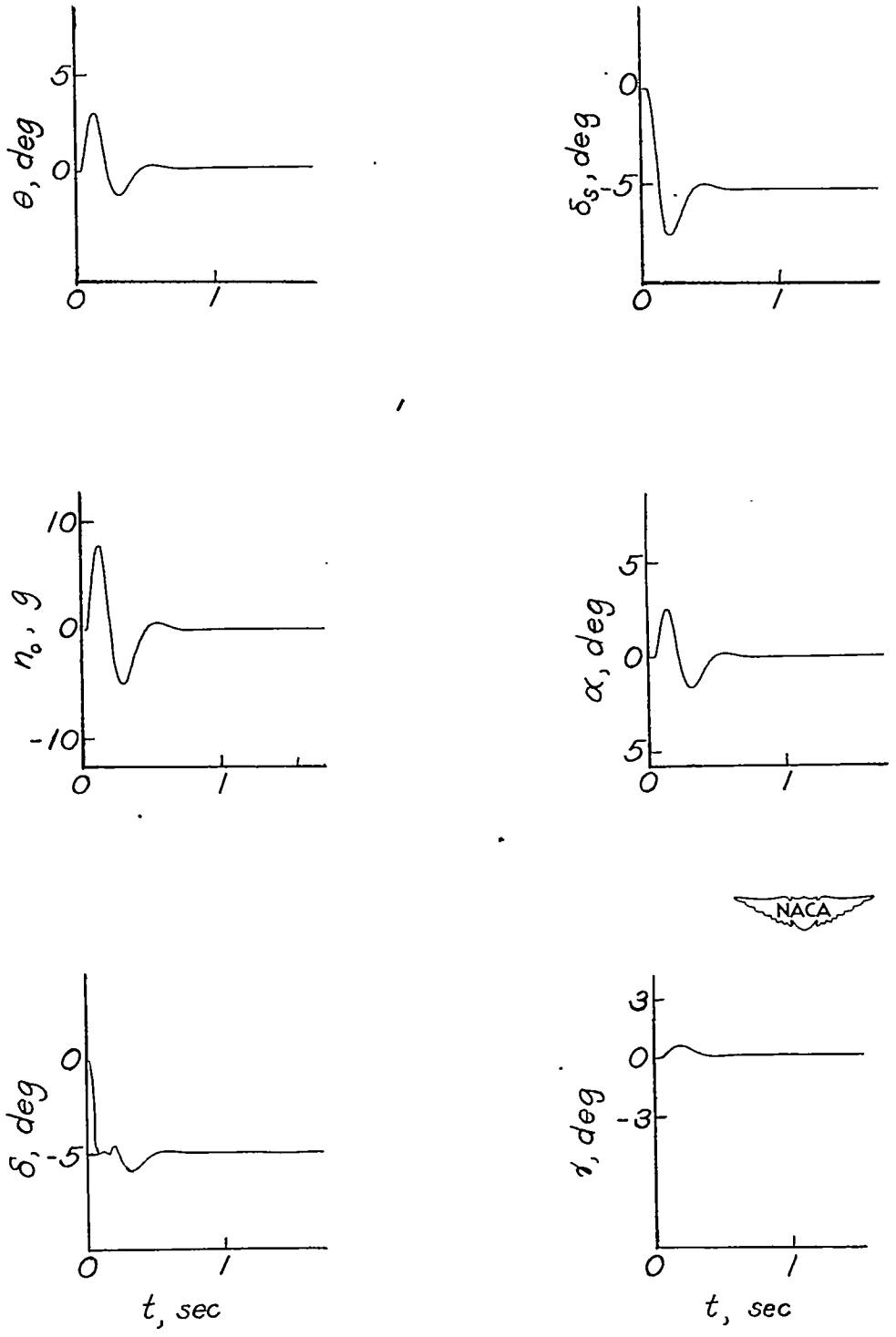

(d) Dead spot equal to 2°.

Figure 7.- Concluded.

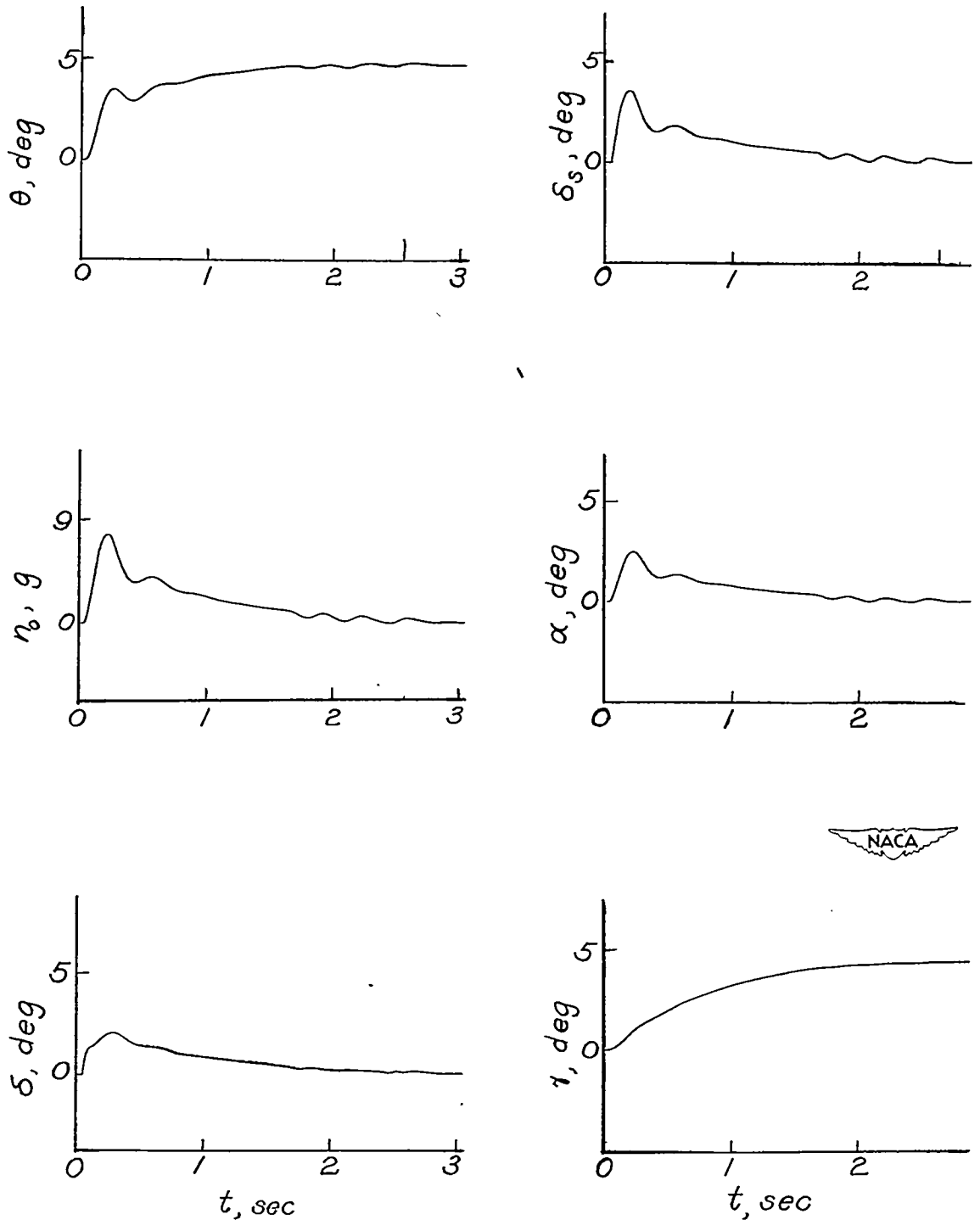

(a) Dead spot equal to 1/2°.

Figure 8.- Effect of dead spot, case II, on missile longitudinal responses subsequent to $\theta_i = 5^\circ$. $K_1 = 120$.

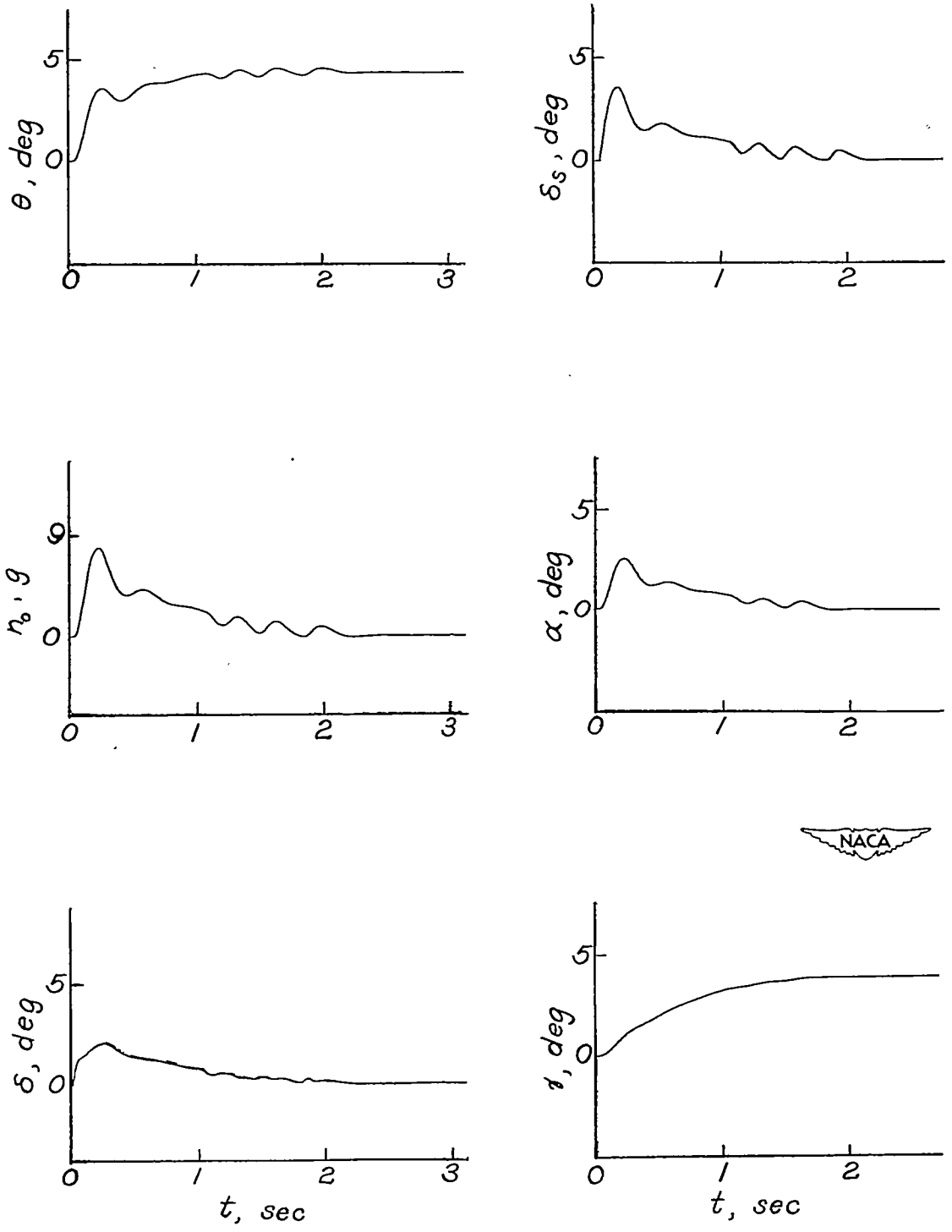

(b) Dead spot equal to 1°.

Figure 8.- Continued.

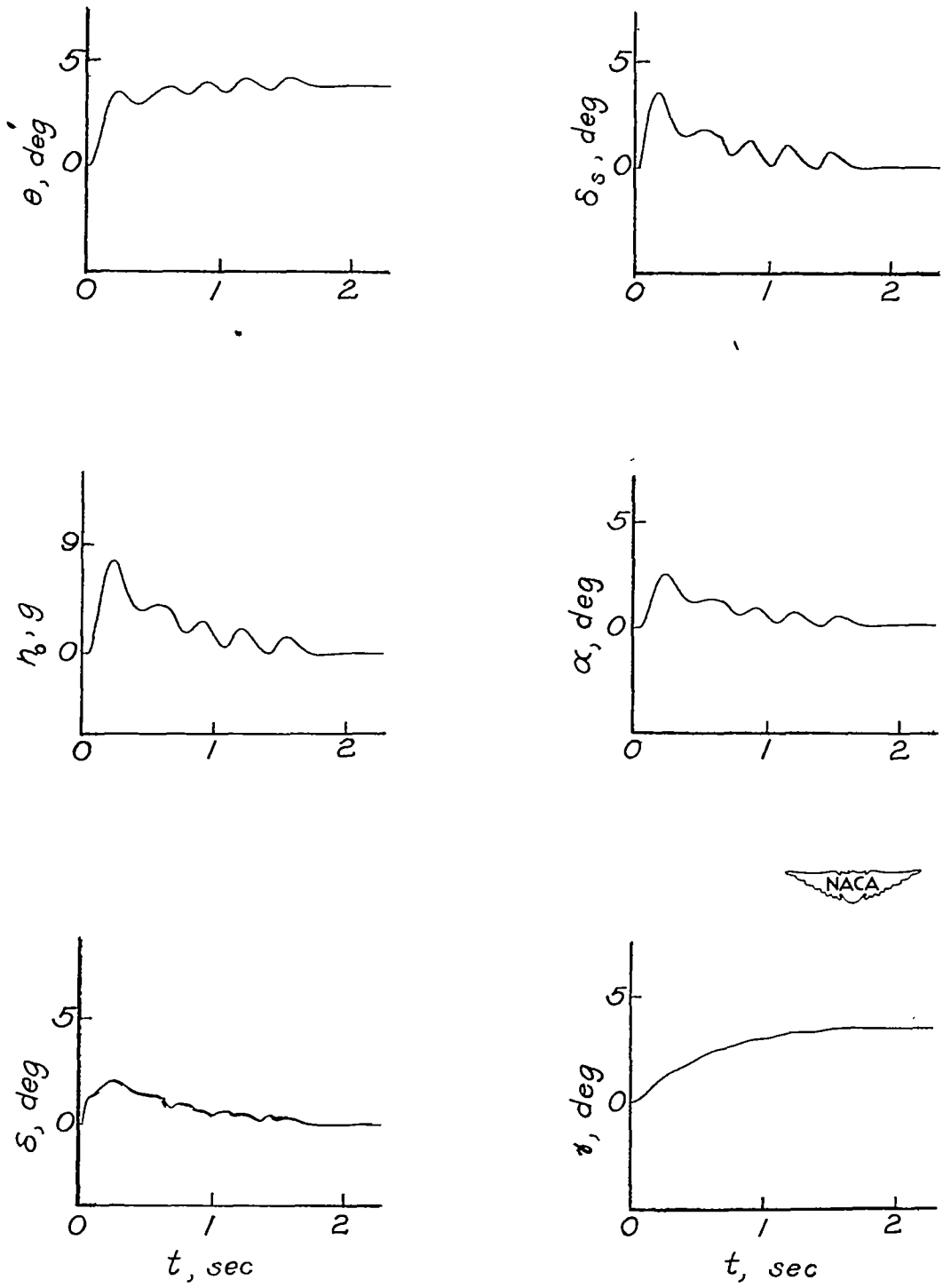

(c) Dead spot equal to $1\frac{1}{2}^{\circ}$.

Figure 8.- Continued.

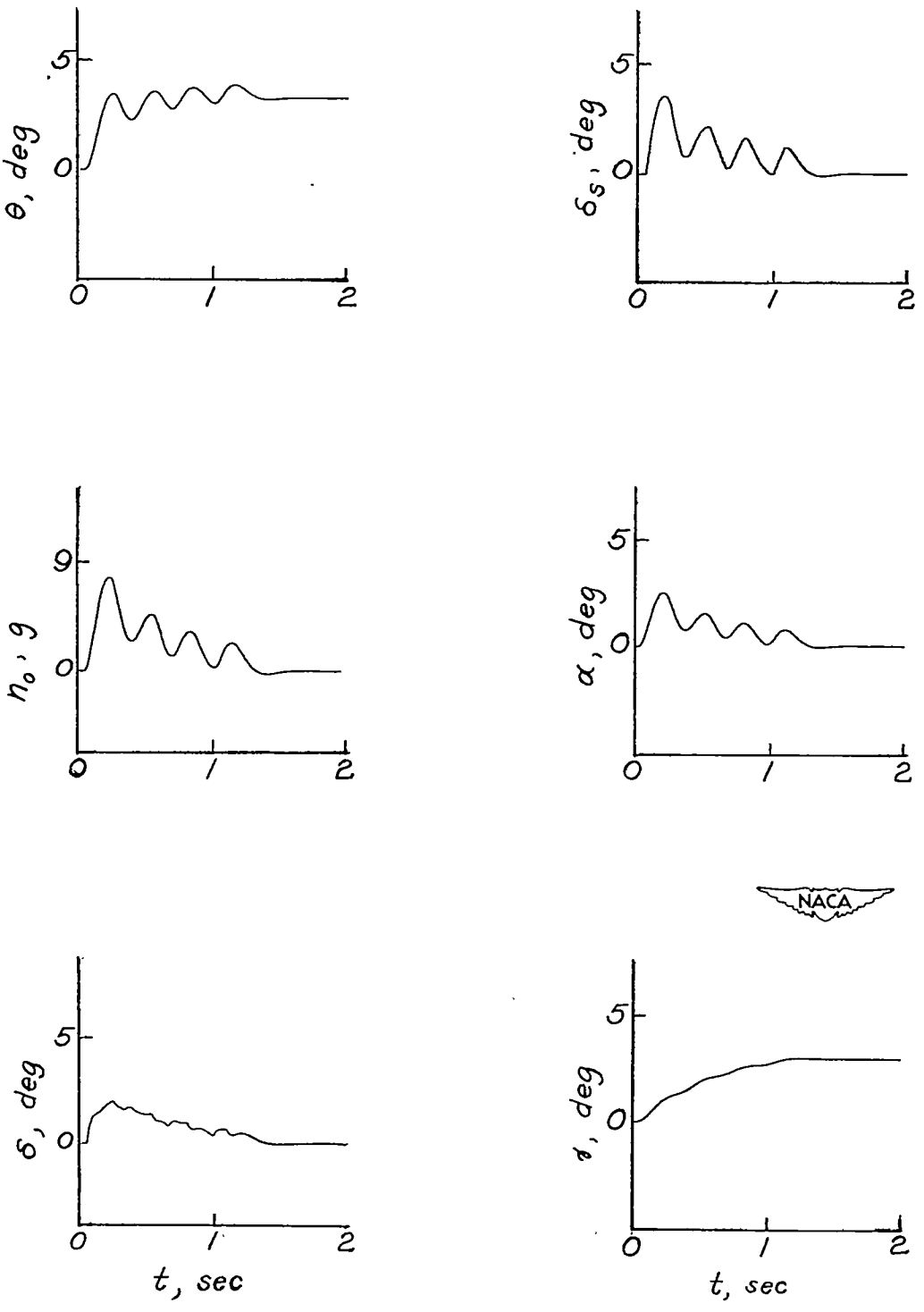

(d) Dead spot equal to 2°.

Figure 8.- Concluded.

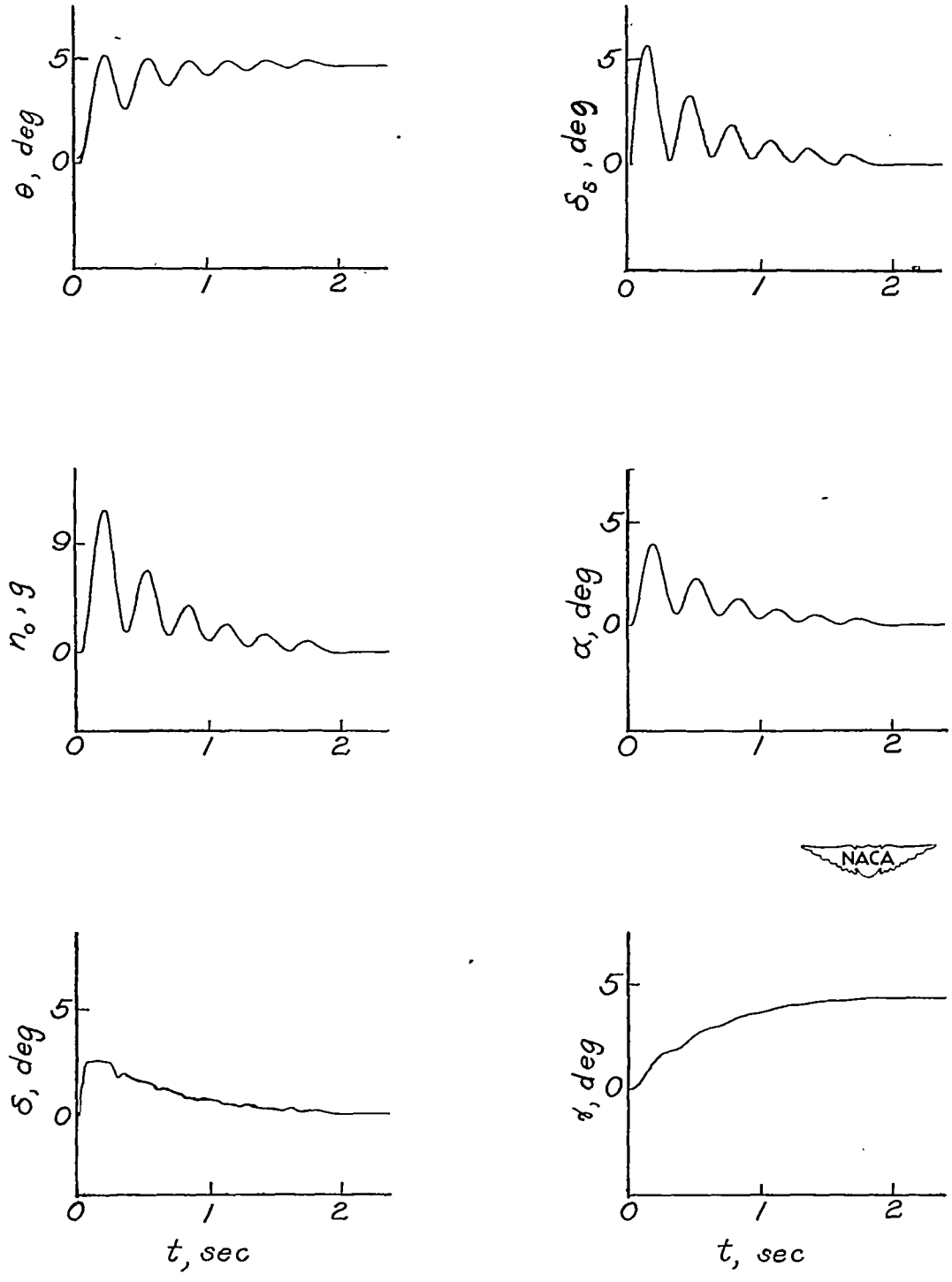

(a) Dead spot equal to 1/2°.

Figure 9.- Effect of dead spot, case II, on missile longitudinal responses subsequent to $\theta_i = 5^\circ$. $K_1 = 225$.

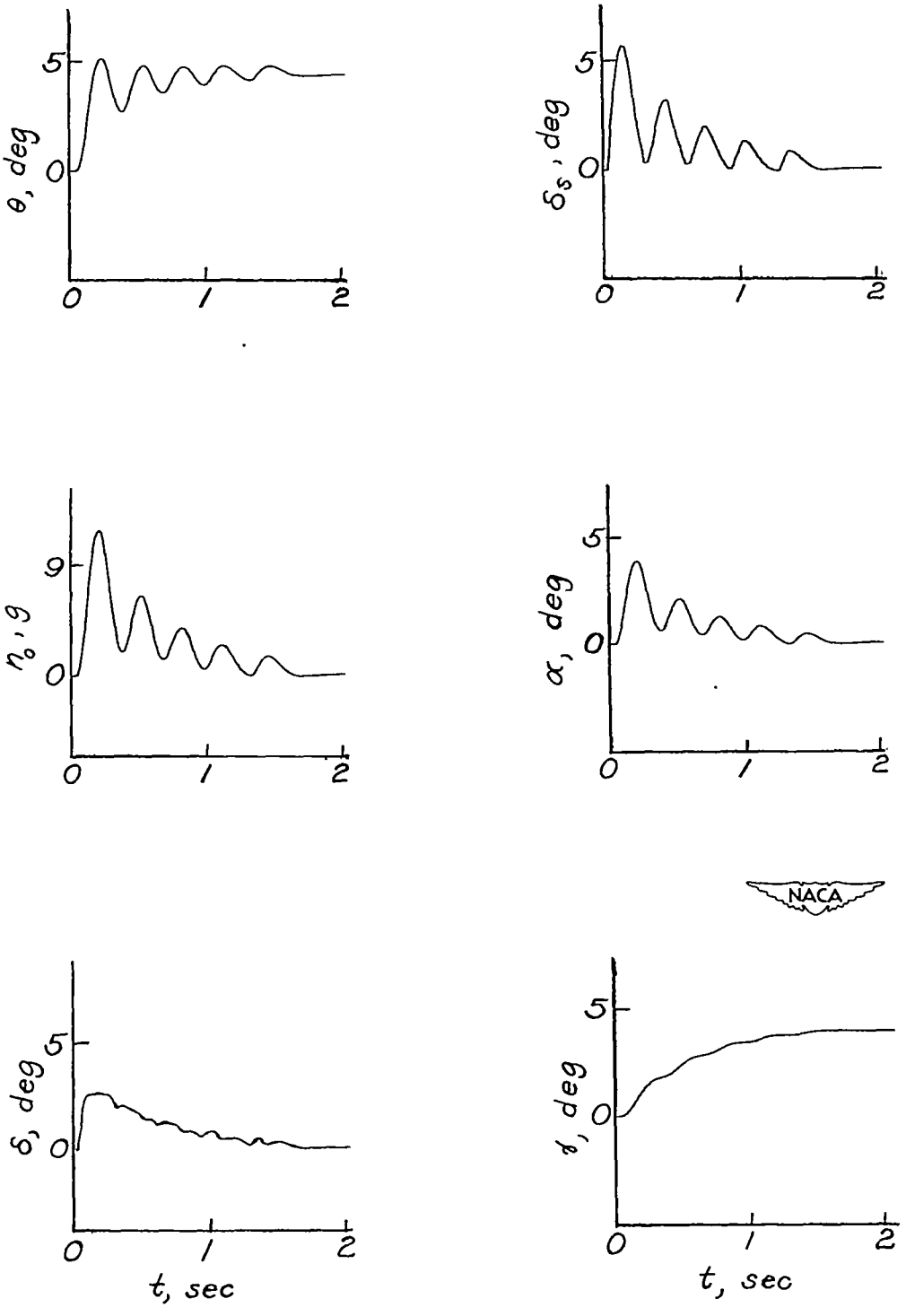

(b) Dead spot equal to 1°.

Figure 9.- Continued.

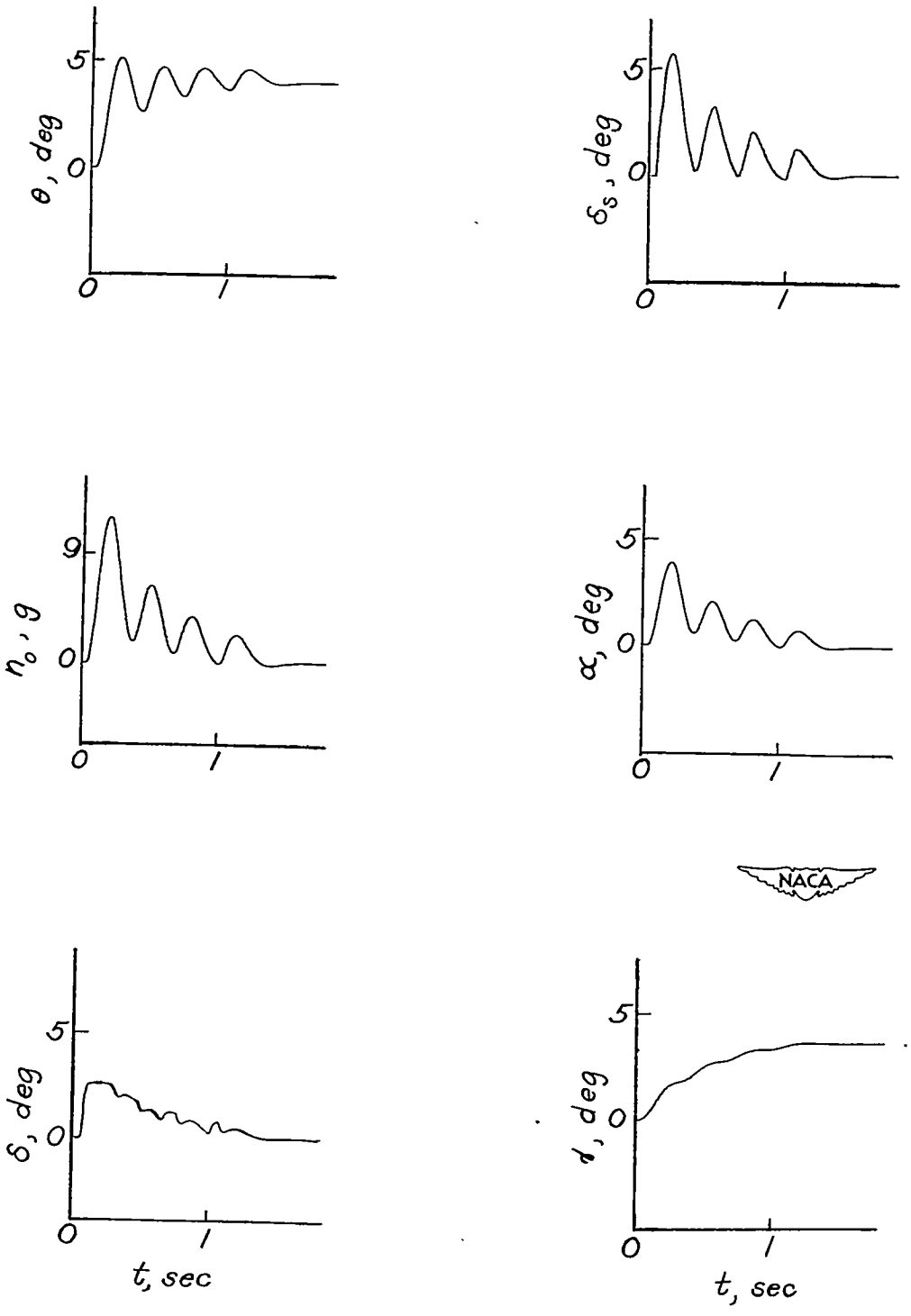

(c) Dead spot equal to $1\frac{1}{2}^{\circ}$.

Figure 9.- Continued.

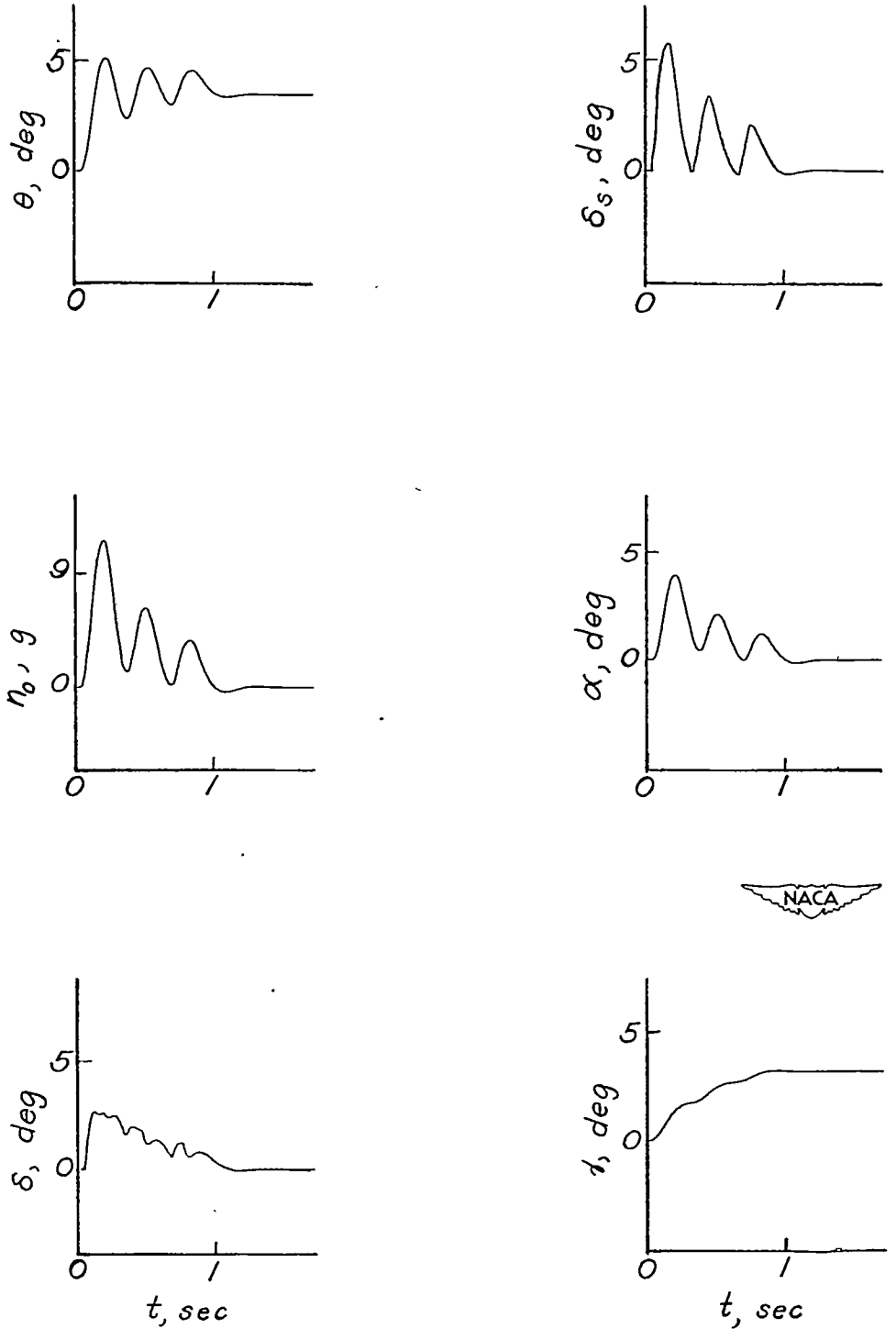

(d) Dead spot equal to 2°.

Figure 9.- Concluded.

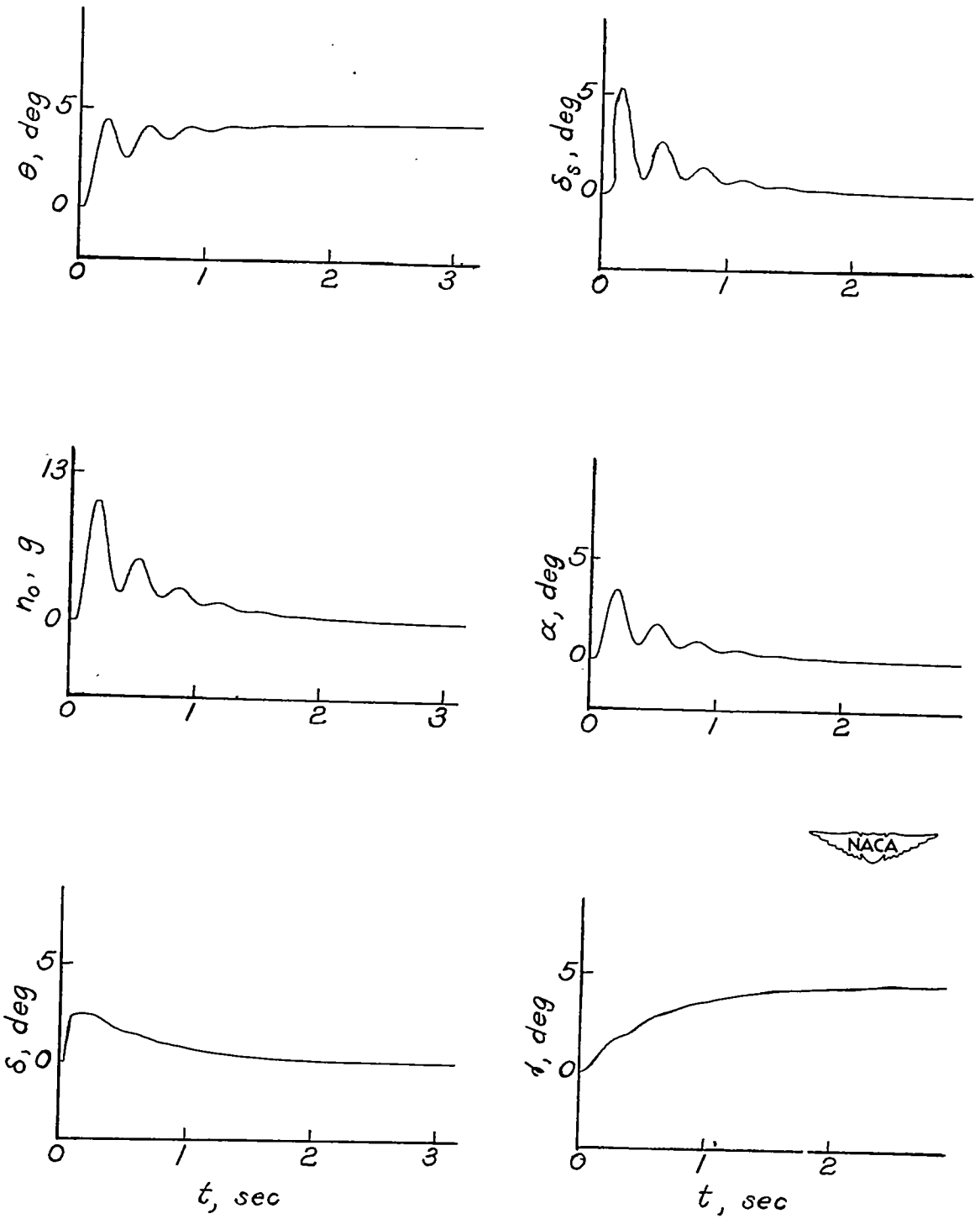

(a) Dead spot equal to 1/2°.

Figure 10.- Effect of dead spot, case III, on missile longitudinal responses subsequent to the command input $\theta_i = 5^\circ$. $K_1 = 225$; $K_1' = 0$; $\tau = 0$.

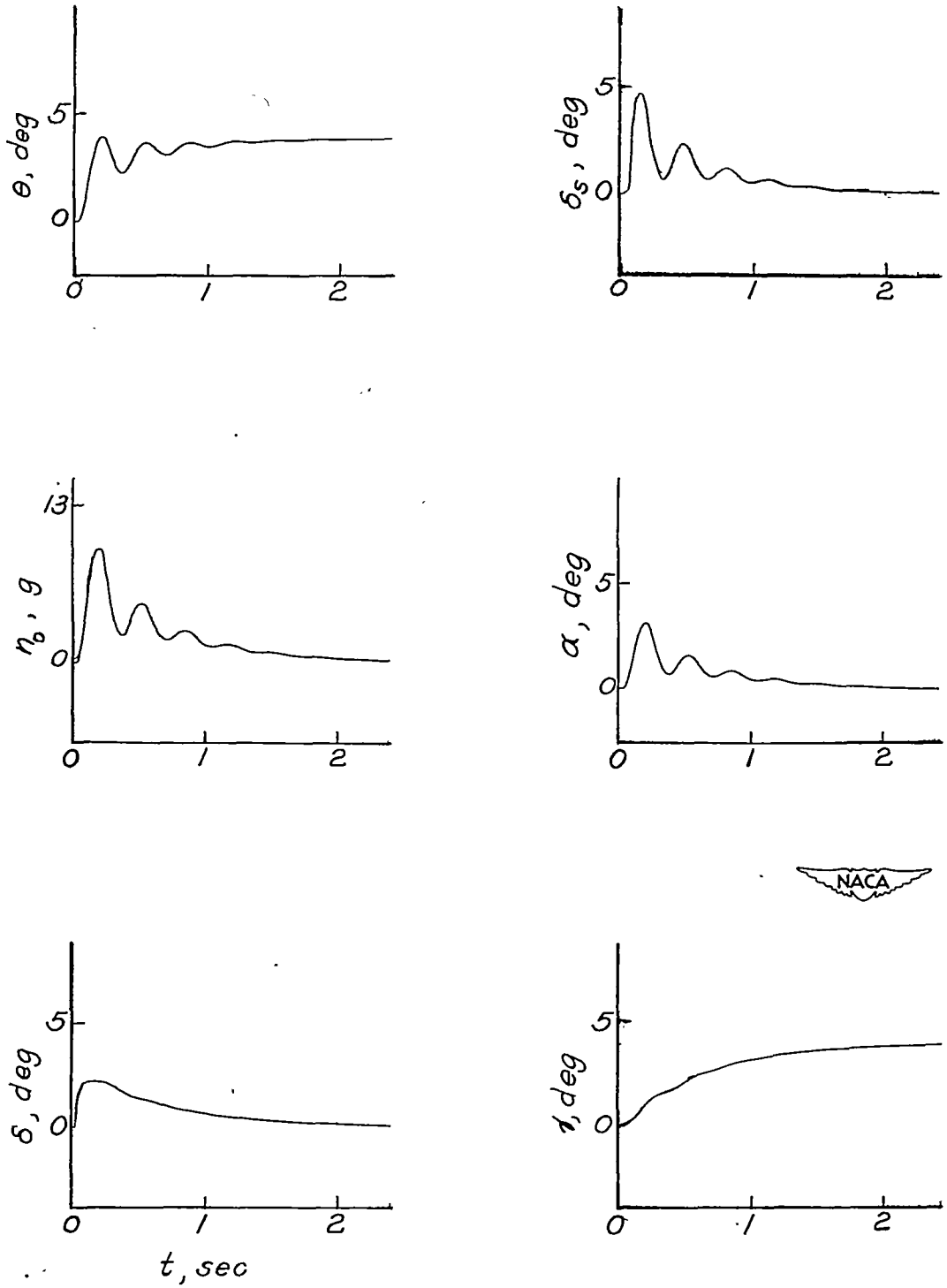

(b) Dead spot equal to 1°.

Figure 10.- Continued.

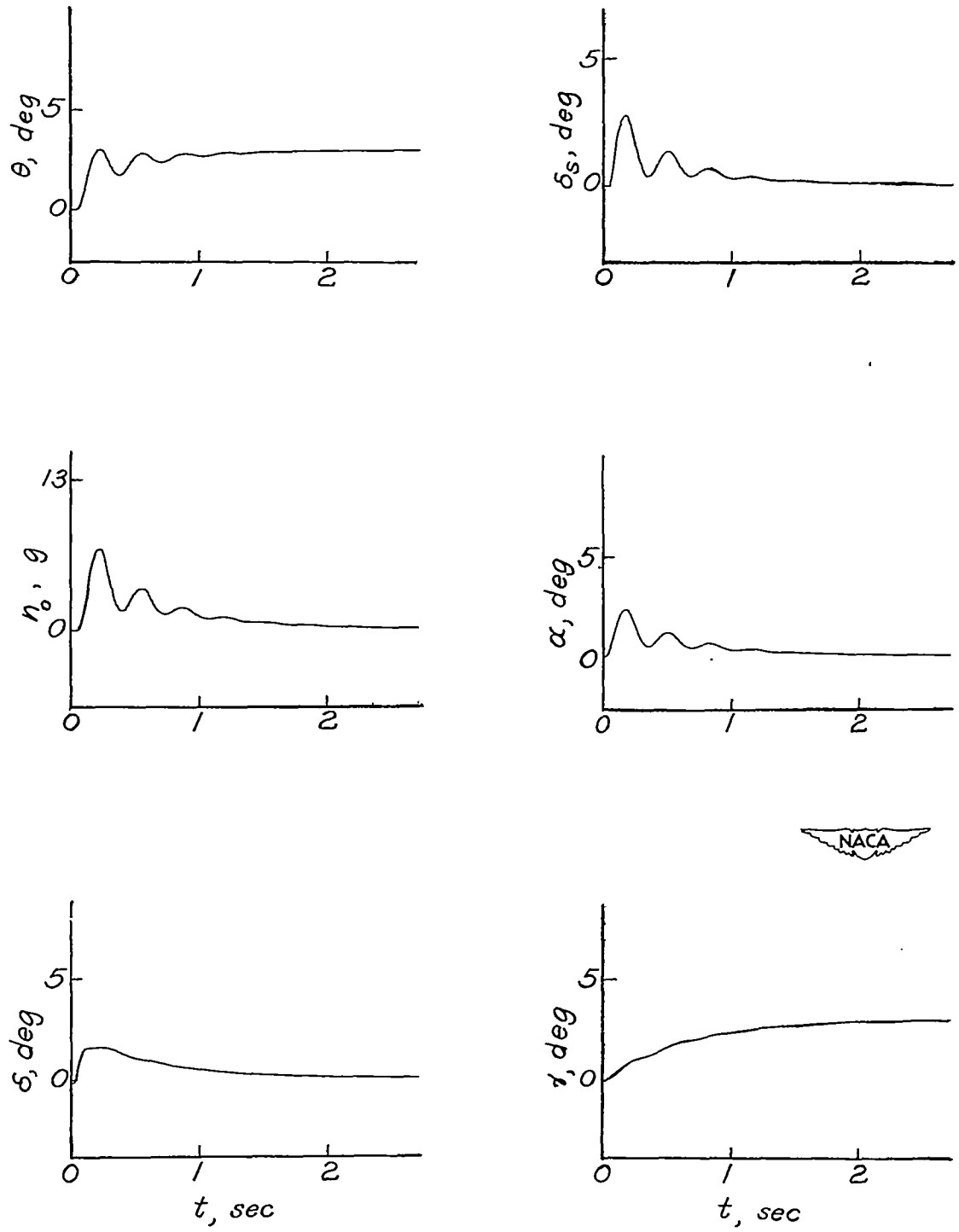

(c) Dead spot equal to 2°.

Figure 10.- Concluded.

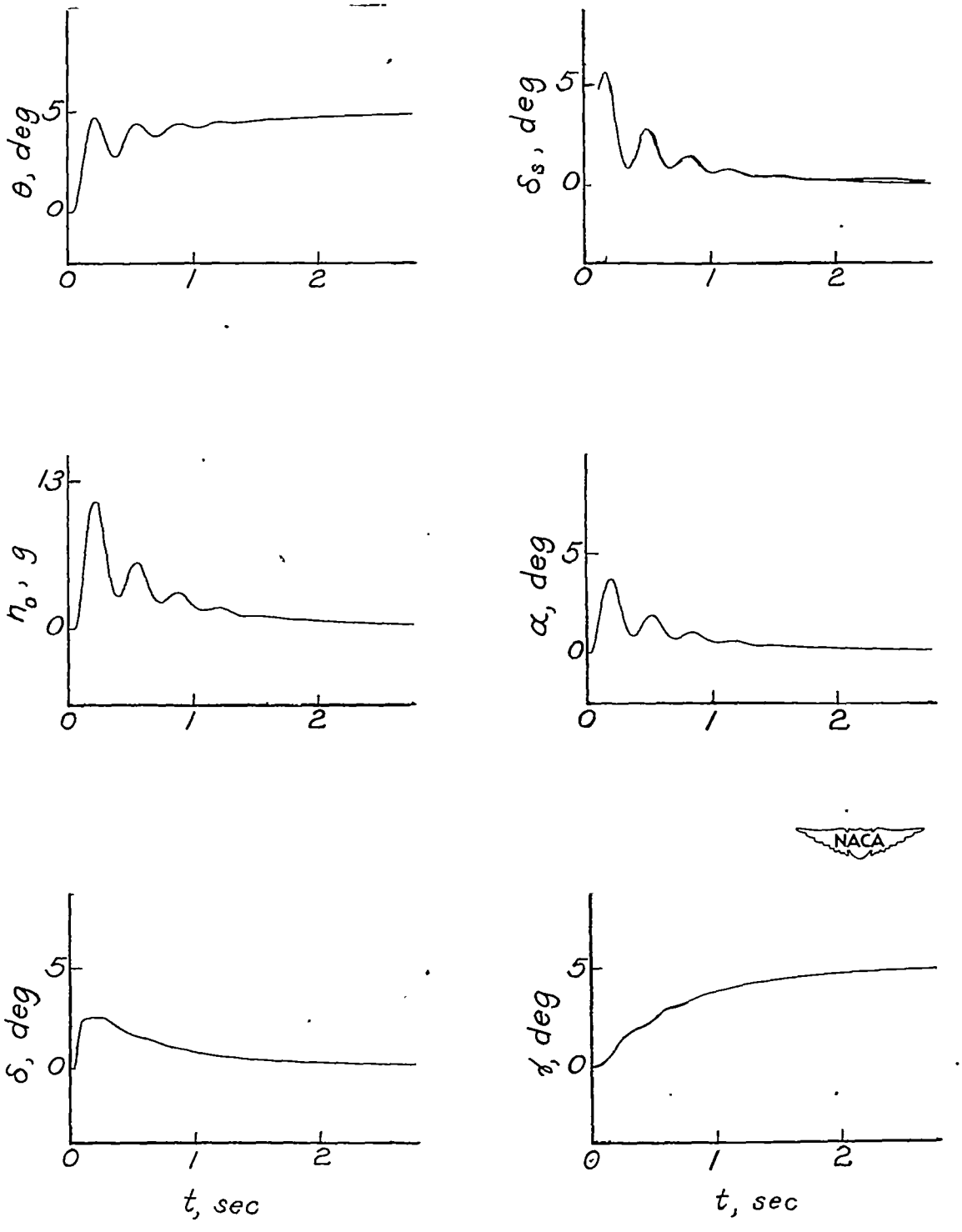

(a) Dead spot equal to 1/2°.

Figure 11.- Effect of dead spot, case IV, on missile longitudinal responses subsequent to the command $\theta_i = 5^\circ$. $K_1 = 225$, $K_1' = \frac{K_1}{2}$; $\tau = 0$.

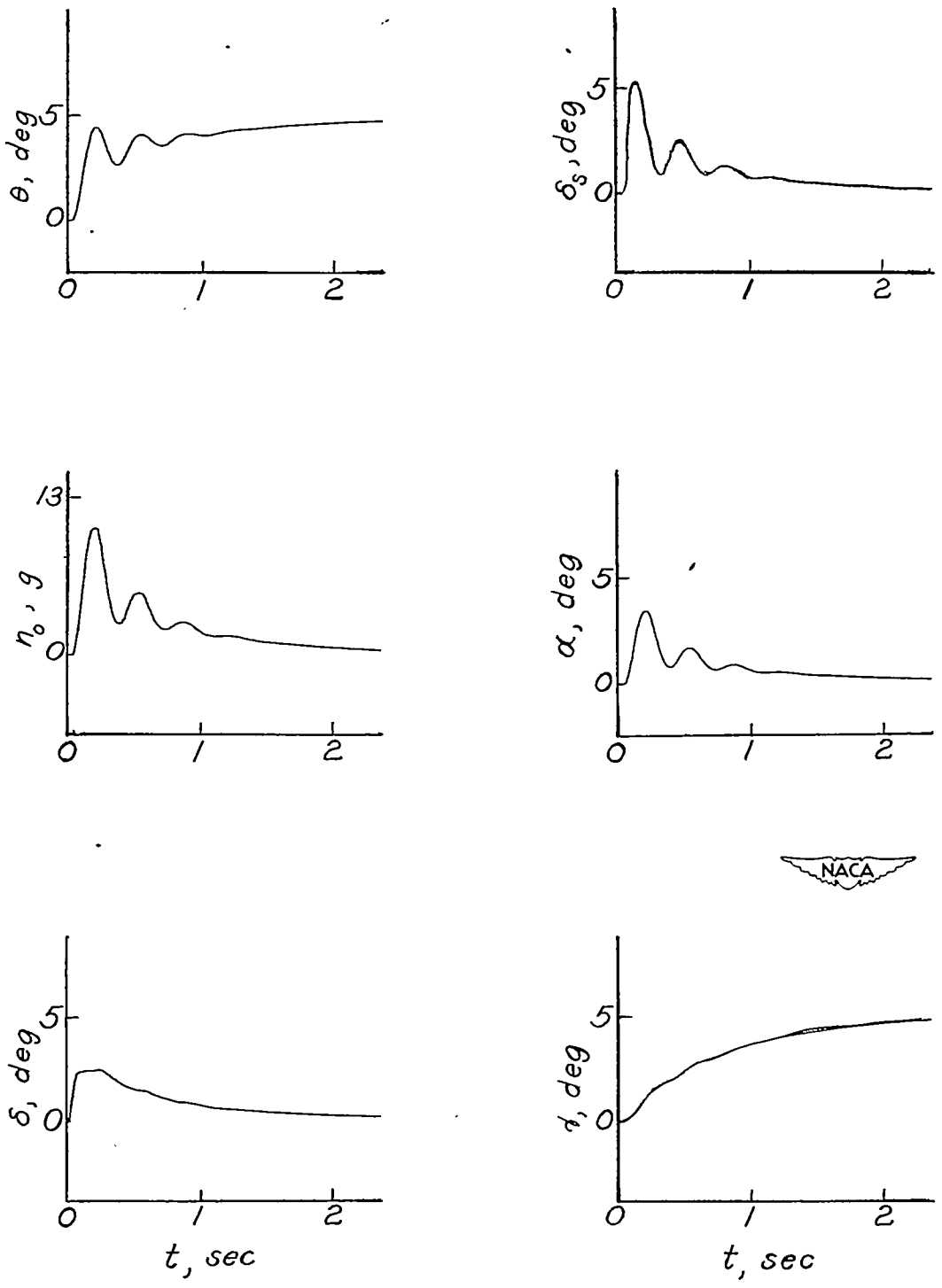

(b) Dead spot equal to 1°.

Figure 11.- Continued.

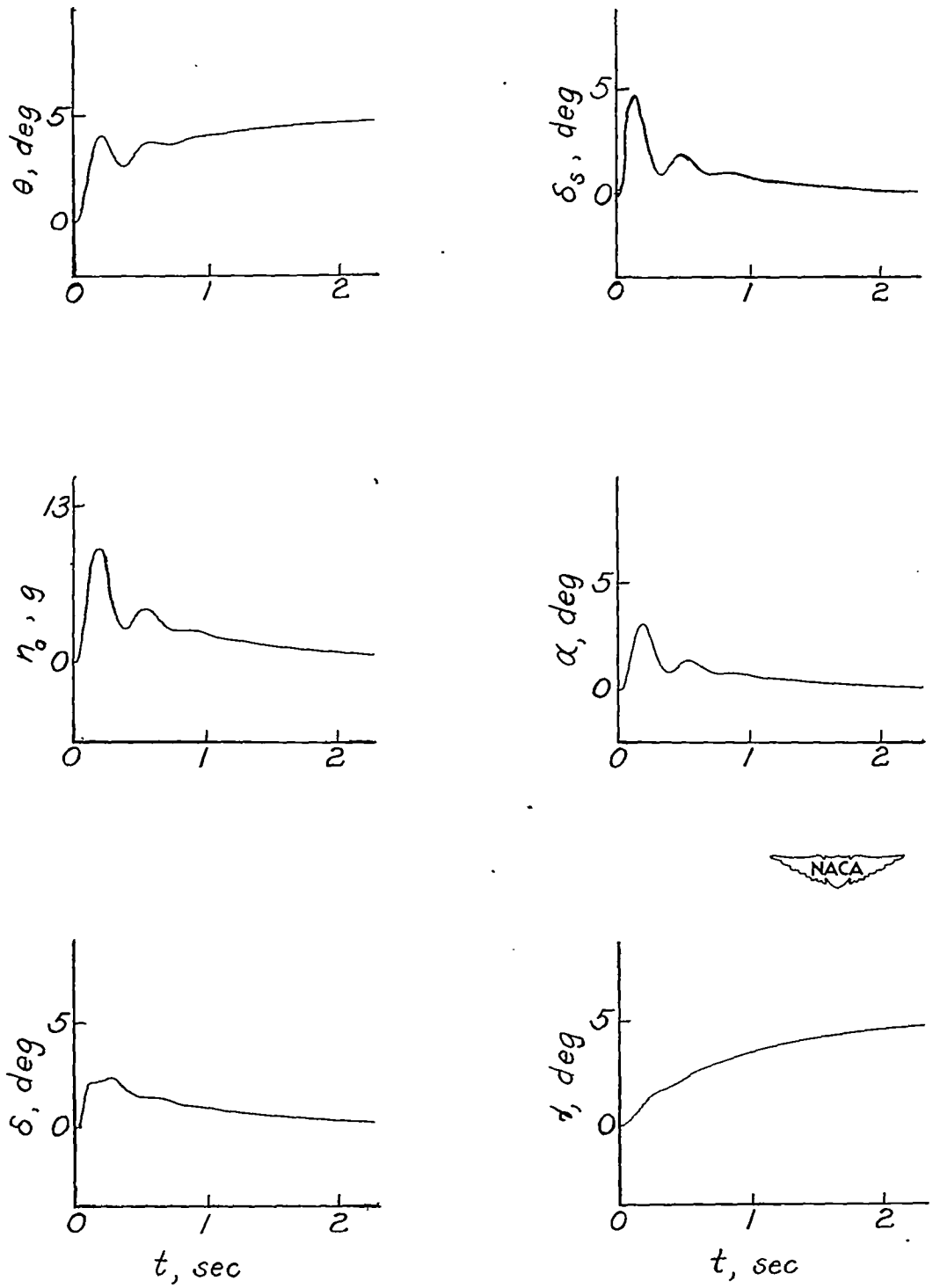

(c) Dead spot equal to 2°.

Figure 11.- Concluded.

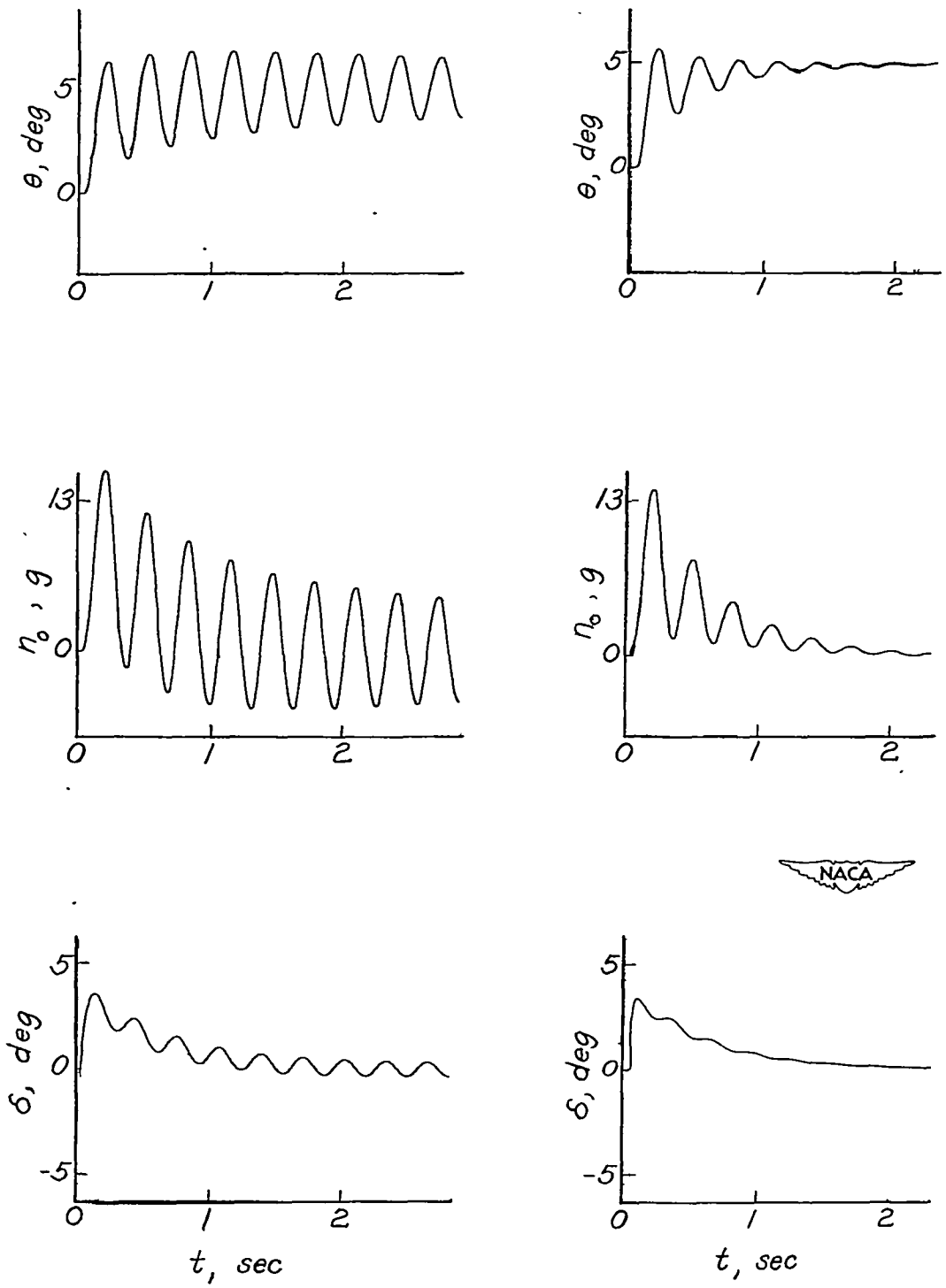

(a) Rate-block dynamics neglected. (b) Rate-block dynamics included.

Figure 12.- Comparison of missile longitudinal motions for $\frac{\delta_R}{D\theta} = \frac{518}{D^2 + 88D + 774}$ and $\frac{\delta_R}{D\theta} = 0.067$. $K_1 = 300$.

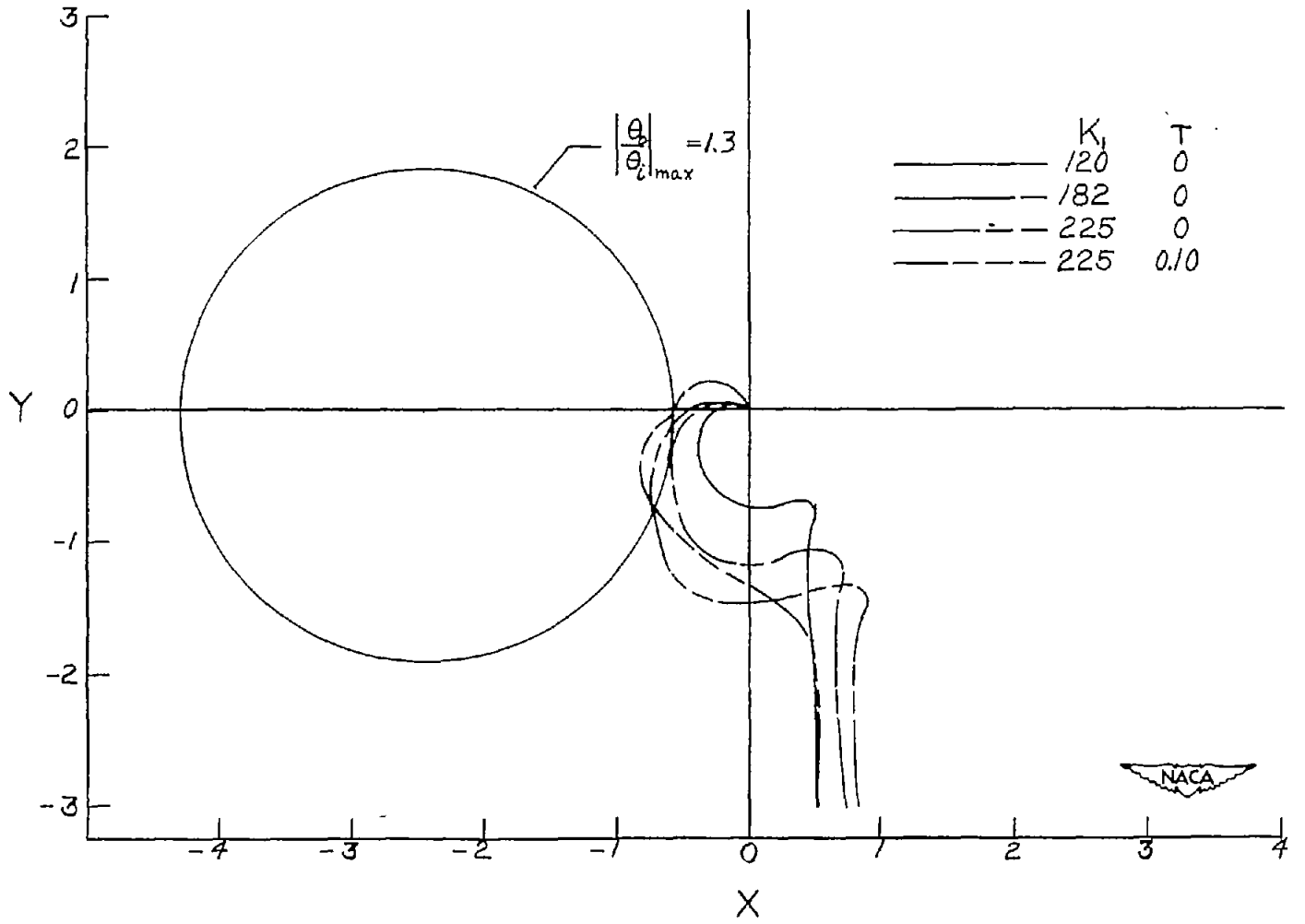

Figure 13.- Comparison of the missile open-loop frequency response $\frac{\theta_o}{\epsilon_1}(i\omega)$ for several values of the target-seeker gain constant K_1 and time constant τ.

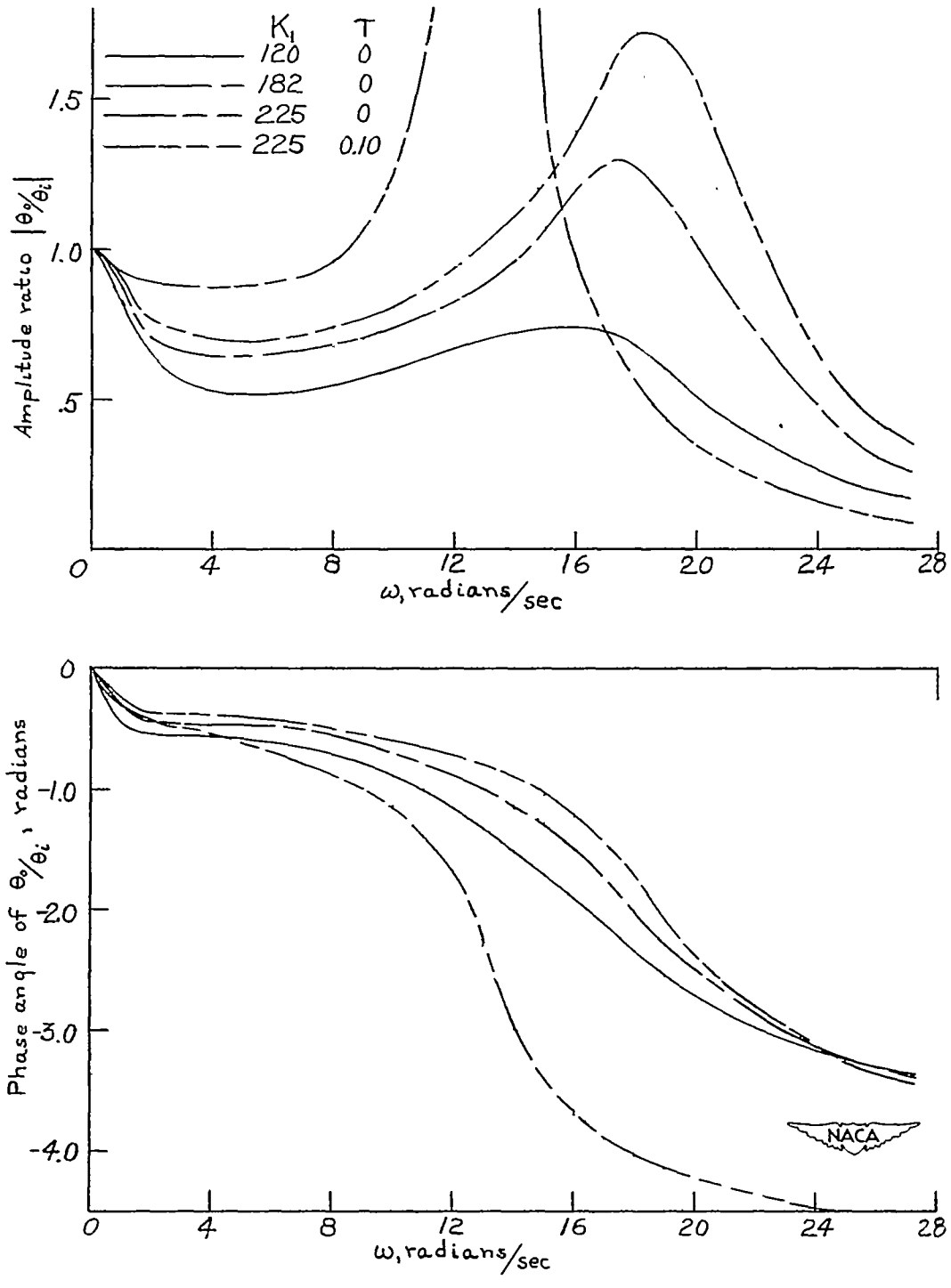

Figure 14.- Comparison of the missile closed-loop frequency response $\frac{\theta_o}{\theta_i}(i\omega)$ for several values of the target-seeker gain constant K_1 and time constant τ.

NACA-Langley - 8-26-52 - 350